Thermochimica Acta 753 (2025) 180143

Contents lists available at ScienceDirect

Thermochimica Acta

journal homepage: www.elsevier.com/locate/tca

Recognition of the thermal dissociation/denaturation mechanisms for multimeric proteins through DSC experiments: a thermodynamic insight

Dimitrios Fessas, Francesca Saitta *

Department of Food, Environmental and Nutritional Sciences (DeFENS), Università degli Studi di Milano, Via Celoria 2, 20133 Milan, Italy

ARTICLE INFO

Keywords:
Proteins
Multimers
Homomer dissociation
Thermal denaturation
Thermodynamic models
Differential scanning calorimetry

ABSTRACT

The importance of knowing the conformational structure of a protein and the related mechanism of denaturation stems from the crucial role that these macromolecules perform in the biological world, and hence the wide spectrum of possible applications in the frame of biological and pharmaceutical research activities. However, in a biological context where a significant number of proteins exists as multimers, stand-alone thermodynamic equations able to simulate and fit Differential Scanning Calorimetry (DSC) profiles involving dissociation phenomena are still missing: different valuable models have been reported in the literature since the 1980s but all were based on the application of experimental protein conversion fractions from the native to the dissociated/denatured state.

In this frame, the present work develops thermodynamic equations that are completely independent of experimental data and are related to three main models: *i)* $N_n \leftrightarrow nD$; *ii)* $N_n \leftrightarrow nM \leftrightarrow nD$; *iii)* $N_n \leftrightarrow I_n \leftrightarrow nD$. Beside inspecting the influence of each fitting parameter on the theoretical $C_p(T)$ curve for the single models, two applications to experimental results are also discussed.

Furthermore, aiming at simplifying the application of thermodynamic equations to proteins of biological and/or pharmaceutical interest, the work develops extensively the solutions for all the models considering the most common homomers, *i.e.*, dimers, trimers, and tetramers.

The methodology and strategy proposed here, that link statistical mechanics concepts (canonical partition function) with the classical thermodynamics' equilibrium constant, are general and pave the way for the development of models that may reflect more complex scenarios than those considered in this work, if the case.

1. Introduction

Proteins act as main characters in most of the biological processes related to the normal physiological activity of living organisms, such as cell signalling, gene expression and control, *etc.* [1] as well as to the onset and progression of several pathologies of enormous social impact, such as cancer, neuropathies, and viral diseases [2–5]. For this reason, many efforts are devoted to the achievement of knowledge about the protein native conformations and the "forces" that stabilize the protein in a specific environment [6–8].

Especially for globular proteins, the conformational structure acquired by the proteins in their native state during the folding process among other structural possibilities has been shown to be driven by many features, such as surface hydrophobicity, local distribution of hydrophilic and hydrophobic amino acid residues, presence of internal structural cavities and their interaction with water molecules [9–12]. Often the protein native conformation can involve multiple domains that may behave differently in terms of functionality and/or susceptibility to denaturation, all aspects that are often linked to the thermodynamic properties of the protein itself [13–15].

The depicted scenario is also more complex if we realize that a large cut of proteins with known structure (about 30–50 %) has a natural tendency to self-associate into multimers, mostly existing as homomers, *i.e.*, homo-oligomeric protein complexes composed of two or more identical subunits [16,17]. In addition, even roughly 45 % and 60 % of eukaryotic and prokaryotic proteins, respectively, that are deposited in data banks as single polypeptide chains also exist as homomers [18]. Such a tendency has been hypothesised and established to be related to possible advantages arising from the association of monomeric units, such as the achievement of a "closed structures" with an intrinsic symmetry and probably an enhanced stability [19,20]. In particular, the potential advantages of being a multimeric protein in living systems

* Corresponding author.
E-mail address: francesca.saitta@unimi.it (F. Saitta).

https://doi.org/10.1016/j.tca.2025.180143
Received 1 August 2025; Received in revised form 25 September 2025; Accepted 26 September 2025
Available online 27 September 2025
0040-6031/© 2025 The Authors. Published by Elsevier B.V. This is an open access article under the CC BY license (http://creativecommons.org/licenses/by/4.0/).

have been mainly identified as: genetic saving, that relies on both the energy save and the reduced probability of errors during gene replication encountered by cells when synthetizing small monomeric units rather than large polypeptide chains; functional gain, intended as any enhancement in the efficiency of the biological action upon oligomerization; structural advantage, that, among others, is related to the ability of finely tuning the protein (often enzyme) activity through subtle conformational changes more easily allowed in multimers [16,21].

In this context, High-Sensitivity Differential Scanning Calorimetry (HS-DSC) has been widely applied to assess the energetic landscape and thermodynamic stability that govern protein behaviour, all information that are achievable by studying the protein denaturation phenomenon [22]. Furthermore, throughout the years, the intersection of equilibrium thermodynamics and statistical mechanics have led to the development of methods for the quantitative analysis of the denaturation phenomenon of monomeric proteins [23–25]. In particular, the models developed have produced equations that permit to simulate the calorimetric profiles for those single-standing globular proteins that undergo thermal denaturation, also including and discriminating domain contributions, if multiple domains are present, and/or, in some cases, irreversible phenomena such as protein aggregation (if any) [14,26,27]. These theoretical models are independent and not biased by any experimental parameter: in other words, they permit a fair fitting with the experimental DSC profiles as $C_p^{exc}(T)$ (in excess with respect to the protein native state specific heat capacity), allowing to gain information about the thermodynamic stability and denaturation mechanism of the protein.

On the other hand, much less theoretical progress has been experienced concerning the description of multimeric proteins that undergo thermal denaturation, although several biochemical, spectroscopic, and computational methods were developed in the recent years to assess the protein oligomer structural features [28]. Indeed, even in the simplest case of a multimeric protein undergoing a $N_n \leftrightarrow nD$ equilibrium, where N_n and D indicate the protein native and denatured forms, respectively, the intersection of equilibrium thermodynamics and statistical mechanics is no longer so simple since, apparently, the total number of molecules changes when moving from the native state to the denatured one.

To overcome this difficulty, the most applied quantitative methods for modelling a protein denaturation process with simultaneous multimer dissociation through the years have been based on an approach proposed by Privalov and Potekhin in the 1980's [25], which took advantage of the degree of advancement $\vartheta(T)$ of the experimental calorimetric profile (partial area/total area ratio) for the derivation of a fitting equation based on the classical thermodynamic equilibrium vant'Hoff equation. Nevertheless, although this method is a very useful tool to validate thermodynamic aspects of equilibria involving multimers, the emerged $C_p(T)$ equation to be compared to the experimental calorimetric profile is actually dependent on the experimental data itself (that is ϑ). In other words, this approach is a validation method that always returns a profile that is bound to the experimental data and not a method that permits an independent simulation of the calorimetric curve for a fair fitting of the experimental data.

Conscious of the great importance of recognizing the mechanisms involved in the thermal denaturation of protein multimers, in this work the authors developed independent thermodynamic models for the description of three possible dissociation/denaturation equilibria to fulfil this gap, also critically inspecting the properties of the proposed models. In particular, the approach is based on the same concept of the statistical mechanics' canonical ensemble applied for the development of the quantitative investigation of monomeric proteins undergoing denaturation through an equilibrium mechanisms [23,24] and is applied to the *i)* $N_n \leftrightarrow nD$, *ii)* $N_n \leftrightarrow nM \leftrightarrow nD$, and *iii)* $N_n \leftrightarrow I_n \leftrightarrow nD$ equilibria (being N_n the native multimer, M the dissociated monomer, I_n an intermediate multimer, D the denatured monomer), that are the most common ones according to the literature [16,29]. Furthermore, being aware of the complexity of the general equations encompassed, this work also aims at providing the literature with the solutions and ready-to-use equations for three of the most common homomers, namely dimer N_2, trimer N_3, and tetramer N_4 [16].

2. Methods and models

2.1. General considerations and strategy

The experimental DSC output for protein thermal denaturation, that is normally shown in terms of $C_p^{exc}(T)$ (specific heat capacity in excess with respect to the native state, see Appendix E for details), is commonly expressed per mole of overall protein present in the measurement cell. In the case of a protein that we presume is in a multimeric state, N_n, with n to be defined, it is good practice to express the data per mole of protein monomers, M. The theoretical models developed here are precisely intended to produce an output suitable to fit experimental data normalized per mole of protein monomers.

It is worth noting that the choice of expressing the calorimetric data in terms of monomers is more profound than applying a simple multiplicative factor. As a matter of fact, this way permits a simple development and description of any protein thermal denaturation model involving a dissociation step in terms of statistical mechanics. Indeed, despite the total number of molecules changes during a dissociation process according to the dissociation stoichiometry, the total number of monomers, M_{tot}, remains constant. In this view, we can treat the system of protein monomers as a canonical ensemble of energetic states (which demands the total number of molecules to be constant throughout the process), that is a classical and discrete representation of the system itself: for such an ensemble, the canonical partition function, Q, that is the normalization function that takes into consideration the probability of each possible state the system could be in, can be easily defined [23].

Going into details, whatever the dissociation model assumed is, we can represent all the species in terms of monomers, hence involving for instance native monomers either associated into the multimeric form or dissociated, associated or dissociated monomers in an intermediate state, or also denatured monomers. Being each of these conditions a possible energetic state the monomers can be in, we can always state that $\sum_i n_i = M_{tot}$ by denoting with n_i the number of monomers in the energetic state i.

According to the law of large numbers, the probability P_i of each monomer to be in the i^{th} state coincides with the molar fraction of monomers f_i, that can also be represented as a ratio of molar concentrations when considering solution equilibria like our case:

$$P_i = f_i \equiv \frac{n_i}{M_{tot}} = \frac{[i]}{[M]_{tot}} \tag{1}$$

It is important to note that the possibility of expressing the probabilities as simple ratios of molar concentrations allows us to link the statistical mechanics' equations with the classical thermodynamics' ones, *i.e.*, in terms of classical thermodynamics' equilibrium constants, whose temperature dependence is clear and immediate [30,31].

Indeed, by selecting one specific monomeric condition (*i.e.*, a specific energetic state) as the reference state, the mass balance expressed per molar concentration at a given temperature results

$$[M]_{tot} = [ref] + \sum_{i \neq ref} [i] \tag{2}$$

being $[ref]$ and $[i]$ the molar concentrations of the monomers present in solution in the reference and i^{th} states, respectively, and $[M]_{tot}$ the total molar concentration of the monomers. By dividing each member of the Eq. (2) by the $[ref]$, we obtain the function

$$Q = 1 + \sum_{i \neq ref} \frac{[i]}{[ref]} \tag{3}$$

The function Q defined in Eq. (3) coincides with the canonical partition function of the system, and it is easy to verify that

$$f_{ref} = \frac{1}{Q} \text{ and } f_i = \frac{[i]/[ref]}{Q}, \text{ with } f_{ref} + \sum_{i \neq ref} f_i = 1 \tag{4}$$

being f_{ref} and f_i the molar fraction of the monomers in the reference and i^{th} states, respectively.

The knowledge of the temperature dependence of the partition function $Q(T)$, and in turn of the species distributions through f_{ref} and f_i, would allow to gain the enthalpy variation $\Delta H(T)$ with respect to the reference state and expressed per mole of monomer, and hence also the theoretical specific heat capacity $C_p(T)$ curve

$$C_p(T) = \frac{d\Delta H(T)}{dT} \tag{5}$$

that could be used to fit the experimental data (please note that Eq. (5) does not include the overall intrinsic heat capacity drop, $\Delta_d C_P$, which is not taken into consideration in this work since the corresponding experimental value is often affected by a rather large error and then is generally neglected in the fitting procedures – see Appendix E for further details).

Through the aforementioned connection between statistical mechanics and classical thermodynamics, the temperature dependence of the canonical partition function $Q(T)$ can be obtained by applying the concept of the classical thermodynamics' equilibrium constant $K(T)$, that will be used and integrated to Eq. (3) taking trace of the stoichiometry according to the peculiar dissociation model under investigation.

In this context, we must also acknowledge that the thermodynamic approach discussed only operates under the assumption of quasi-equilibrium DSC experiments, where irreversible kinetic effects are negligible.

2.2. Concomitant multimeric protein dissociation/denaturation equilibrium model

This model considers a multimeric protein N_n in the native state that can undergo, upon heating, a dissociation equilibrium into monomers concurrently with the thermal denaturation of the monomers themselves. For such a situation, the following equilibrium model can be considered as descriptive of the overall process

$$N_n \overset{K}{\leftrightarrow} nD \tag{6}$$

where "D" represents the dissociated monomer in the denatured state and K is the related thermodynamic equilibrium constant given by

$$K \equiv \frac{a_D^n}{a_{N_n}} \approx \frac{[D]^n}{[N_n]} \tag{7}$$

considering that, for properly diluted solutions, the molar concentrations $[N_n]$ and $[D]$ are allowed to replace the thermodynamic activities a_{N_n} and a_D, respectively.

When talking in terms of monomers, we may identify two species in solution, namely the native monomers associated into the multimeric form, "AM" ("associated monomers" belonging to the N_n structure), that we assume as the reference state, and the monomers in the dissociated/denatured state, "D". Following the Eqs. (2) and 3, we have

$$[M]_{tot} = [AM] + [D] \tag{8}$$

and

$$Q = 1 + \frac{[D]}{[AM]} \tag{9}$$

Accordingly, the protein monomeric fraction that exists in the associate state, f_{AM}, and the one that exists in the denatured state, f_D, at a given temperature are given by Eq. (4)

$$f_{AM} = \frac{1}{Q} \text{ and } f_D = \frac{[D]/[AM]}{Q}, \text{ with } f_{AM} + f_D = 1 \tag{10}$$

The enthalpy variation $\Delta H(T)$ with respect to the reference state, *i.e.*, the native "AM", and expressed per mole of monomers is given by

$$\Delta H(T) = f_D \cdot \Delta_{dd} H^\circ \tag{11}$$

being $\Delta_{dd} H^\circ$ the molar standard enthalpy variation associated to the transition (dissociation/denaturation) from the "AM" state to the "D" state.

The temperature-derivative of $\Delta H(T)$ provides the theoretical specific heat capacity $C_p(T)$ curve that can be used to fit the experimental data according to Eq. (5) (see Appendix E).

The equations listed so far contain the $[D]/[AM]$ fraction, that depends on temperature. However, this dependence is unknown at this stage, so it has to be made explicit in terms of the model's fitting parameters. To this purpose, by reminding that $[AM] = n[N_n]$ and from Eqs. (7)–9, we obtain

$$Q = 1 + \frac{K}{n[D]^{n-1}} \tag{12}$$

and f_D becomes

$$f_D = \frac{K}{n[D]^{n-1}} \frac{1}{Q} \tag{13}$$

where $[D]$ is obtainable from the resolution of the related mass balance equation (see Appendix B for details):

$$\frac{n}{K}[D]^n + [D] - n[N_n]_{tot} = 0 \tag{14}$$

The temperature dependence of the equilibrium constant K is obtainable by the well-known solution of the van't Hoff equation:

$$K(T) = K(T_{diss}) \cdot \exp\left[\frac{\Delta H^{vH}}{R}\left(\frac{1}{T_{diss}} - \frac{1}{T}\right)\right] \tag{15}$$

with the dissociation temperature, T_{diss}, defined as the temperature at which half of the multimer population has undergone dissociation/denaturation, that means that $[N_n] = [N_n]_{tot}/2$ at this temperature, and $K(T_{diss})$ obtainable from the mass balance equation as reported in Appendix A.i:

$$K(T_{diss}) = \frac{n^n [N_n]_{tot}^{n-1}}{2^{n-1}} \tag{16}$$

Instead, ΔH^{vH} is the standard enthalpy variation associated to the entire process (dissociation/denaturation) expressed per mole of multimer N_n being the K referred to the equilibrium in Eq. (6).

By applying this approach and developing the model for the various dissociation stoichiometries n of interest, different sets of equations are determined, allowing to achieve the theoretical specific heat capacity $C_p(T)$ curves given by the Eq. (5) and needed when attempting the fitting of a DSC trace. In any case, the only fitting parameters for this specific model are T_{diss} and ΔH^{vH}, being $\Delta_{dd} H^\circ = \Delta H^{vH}/n$.

The final equations for the model accounting for the most common multimeric systems, namely N_2, N_3, and N_4 proteins, are shown explicitly in Appendix B and can be easily transferred to a spreadsheet to obtain the theoretical specific heat capacity $C_p(T)$ curve for each case, so to be used for the fitting of the DSC thermograms.

It is worth to note that, although the equations to obtain $[D]$ and $K(T_{diss})$ contain $[N_n]_{tot}$ as a parameter, this term is actually cancelled through the substitution of the solutions to the overall equations that lead to the f_{AM} and f_D as shown in Appendix B, and the population fractions are actually independent of the total protein concentration as expected for an equilibrium process.

As an example, the final equations for $n = 2$ are listed below (see Appendix B for details):

$$Q = 1 + \frac{1}{2D'} \quad - \quad \text{with } D' = \frac{-1 + \sqrt{1 + \frac{8}{K'}}}{4} \text{ and } K' = \exp\left[\frac{\Delta H^{vH}}{R}\left(\frac{1}{T_{diss}} - \frac{1}{T}\right)\right] \tag{17}$$

$$f_{AM} = \frac{1}{Q} \text{ and } f_D = \frac{1}{2D'Q} \tag{18}$$

$$C_p(T) = \frac{d\Delta H(T)}{dT}, \text{ with } \Delta H(T) = f_D \cdot \Delta_{dd}H^\circ \text{ and } \Delta_{dd}H^\circ = \frac{\Delta H^{vH}}{2} \tag{19}$$

where T_{diss} and ΔH^{vH} are the only fitting parameters.

2.3. Multimeric protein dissociation with consecutive denaturation equilibrium model

Although the most common behaviour shown by a multimeric protein is a simultaneous temperature-dependent dissociation/denaturation equilibrium (described by the model reported above), some proteins characterized by more labile association among monomers may exhibit dissociation before the actual thermal denaturation process. Such a scenario needs to consider two distinct equilibria, namely a dissociation equilibrium prior the thermal denaturation one, according to the following scheme

$$N_n \overset{K_{diss}}{\leftrightarrow} nM \overset{K_d}{\leftrightarrow} nD \tag{20}$$

being K_{diss} and K_d the thermodynamic equilibrium constants related to the specific step and given by

$$K_{diss} \equiv \frac{a_M^n}{a_{N_n}} \approx \frac{[M]^n}{[N_n]} \text{ and } K_d \equiv \frac{a_D}{a_M} \approx \frac{[D]}{[M]} \tag{21}$$

considering that, for properly diluted solutions, the molar concentrations $[N_n]$, $[M]$, and $[D]$ are allowed to replace the thermodynamic activities a_{N_n}, a_M, and a_D, respectively.

By representing all the species in terms of monomers, the equilibria considered in Eq. (20) involve:

- "*AM*" as the native monomer associated into the multimeric form $N_n$to be considered as the reference state;
- "*M*" as the dissociated (free) monomer;
- "*D*" as the denatured monomer.

For the mass balance equation, we obtain

$$[M]_{tot} = [AM] + [M] + [D] \tag{22}$$

According to Eq. (3), the partition function Q taking the native "*AM*" state of the protein as a reference simply becomes

$$Q = 1 + \frac{[M]}{[AM]} + \frac{[D]}{[AM]} \tag{23}$$

Accordingly, the monomer fraction that exists in the associated native state, f_{AM}, the one that exists in the dissociated native state, f_M, and the one that exist in the denatured state, f_D, at a given temperature can be written as

$$f_{AM} = \frac{1}{Q}, \; f_M = \frac{[M]/[AM]}{Q}, \text{ and } f_D = \frac{[D]/[AM]}{Q}, \text{ with } f_{AM} + f_M + f_D = 1 \tag{24}$$

Therefore, the overall enthalpy variation $\Delta H(T)$ of the whole process with respect to the reference state, *i.e.*, "*AM*", becomes

$$\Delta H(T) = f_M \cdot \Delta_{diss}H^\circ + f_D \cdot (\Delta_{diss}H^\circ + \Delta_d H^\circ) \tag{25}$$

being $\Delta_{diss}H^\circ$ the standard enthalpy variation associated to the dissociation event from the "*AM*" to the "*M*" state, and $\Delta_d H^\circ$ the standard enthalpy variation associated to the denaturation transition from the "*M*" to "*D*" state. All these enthalpy variations are expressed per mole of the total monomers.

The temperature-derivative of $\Delta H(T)$ provides the theoretical specific heat capacity $C_p(T)$ curve that can be used to fit the experimental data. Hence, by following the same strategy described above to make the temperature-dependence of the $[M]/[AM]$ and $[D]/[AM]$ ratios explicit in terms of the model's fitting parameters, we obtain through Eqs. (21)–23

$$Q = 1 + \frac{K_{diss}}{n[M]^{n-1}} + \frac{K_{diss} \cdot K_d}{n[M]^{n-1}} \tag{26}$$

whereas the respective f_{AM}, f_M, and f_D fractions can be obtained as

$$f_{AM} = \frac{1}{Q}, \; f_M = \frac{K_{diss}}{n[M]^{n-1}} \cdot \frac{1}{Q}, \text{ and } f_D = \frac{K_{diss} \cdot K_d}{n[M]^{n-1}} \cdot \frac{1}{Q} \tag{27}$$

where $[M]$ is obtainable from the resolution of the related mass balance equation (see Appendix C for details):

$$\frac{n}{K_{diss}}[M]^n + (1 + K_d)[M] - n[N_n]_{tot} = 0 \tag{28}$$

Again, the temperature dependence of both the equilibrium constants is obtainable by the well-known solution of the van't Hoff equation. In particular, for the dissociation equilibrium we have

$$K_{diss}(T) = K_{diss}(T_{diss}) \cdot \exp\left[\frac{\Delta H^{vH}}{R}\left(\frac{1}{T_{diss}} - \frac{1}{T}\right)\right] \tag{29}$$

where T_{diss} is the dissociation temperature having the same meaning described in Eq. (15) for the above model, ΔH^{vH} is the enthalpy variation involved in the dissociation step expressed per mole of multimer N_n (since K_{diss} is referred to the first equilibrium in Eq. (20)), and (see Appendix A.ii for details)

$$K_{diss}(T_{diss}) = \frac{n^n [N_n]_{tot}^{n-1}}{2^{n-1}} \cdot \frac{1}{[1 + K_d(T_{diss})]^n} \tag{30}$$

Instead, for the denaturation equilibrium we have

$$K_d(T) = \exp\left[\frac{\Delta_d H^\circ}{R}\left(\frac{1}{T_d} - \frac{1}{T}\right)\right] \tag{31}$$

being $\Delta_d H^\circ$ the denaturation enthalpy defined as above (*i.e.*, the transition from the "*M*" dissociated state to the "*D*" state) and T_d the denaturation temperature. Here we underline that we use the common definition for the denaturation temperature, that is the temperature at which the value $K_d(T_d) = 1$, or in other words, the temperature at which the "*M*" and "*D*" states are equally populated [22,26].

Also for this model, its development for the specific dissociation stoichiometries n of interest provides different sets of equations that allow to achieve the theoretical specific heat capacity $C_p(T)$ curves given by the Eq. (5) and needed to fit a DSC trace. The fitting parameters characterizing this specific model are four (two for each equilibrium), namely T_{diss}, ΔH^{vH}, T_d, and $\Delta_d H^\circ$, being $\Delta_{diss}H^\circ = \Delta H^{vH}/n$.

The final equations for the model accounting for the most common multimeric systems, namely N_2, N_3, and N_4 proteins, are shown explicitly in Appendix C and can be easily transferred to a spreadsheet to

obtain the theoretical specific heat capacity $C_p(T)$ curve for each case, so to be used for the fitting of the DSC thermograms.

Again, it is worth to note that, although the equations to obtain $[M]$ and $K_{diss}(T_{diss})$ contain $[N_n]_{tot}$ as a parameter, this term is actually cancelled through the substitution of the solutions to the overall equations that lead to the f_{AM}, f_M, and f_D as shown in Appendix C, and the population fractions are actually independent of the total protein concentration as expected for equilibrium processes.

As an example, the final equations for $n = 2$ are listed below (see Appendix C for details):

$$Q = 1 + \frac{1}{2M'} + \frac{K_d}{2M'} \tag{32}$$

with $M' = \frac{-(1+K_d)+\sqrt{(1+K_d)^2+\frac{8}{K''_{diss}}}}{4}$ and $K''_{diss} = \frac{1}{[1+K_d(T_{diss})]^2}\cdot\exp\left[\frac{\Delta H^{vH}}{R}\left(\frac{1}{T_{diss}} - \frac{1}{T}\right)\right]$

$$f_{AM} = \frac{1}{Q},\ f_M = \frac{1}{2M'Q},\ \text{and}\ f_D = \frac{K_d}{2M'Q} \tag{33}$$

$$C_p(T) = \frac{d\Delta H(T)}{dT},\ \text{with}\ \Delta H(T) = f_M\cdot\Delta_{diss}H^\circ + f_D\cdot(\Delta_{diss}H^\circ + \Delta_d H^\circ)\ \text{and}\ \Delta_{diss}H^\circ = \frac{\Delta H^{vH}}{2} \tag{34}$$

where T_{diss}, ΔH^{vH}, T_d, and $\Delta_d H^\circ$ are the fitting parameters.

2.4. Partial conformational transition of a multimeric protein with consecutive dissociation/denaturation equilibrium model

Although it might be considered a less frequent situation, it may happen that a multimeric protein N_n undergoes a modification to an intermediate multimeric protein I_n with monomers that are no longer in their native form but still remain in an associated form. Considering that a multimer is often dismantled upon even slight conformational modifications affecting the amino acids of the protein association core, a "preliminary" transition from N_n to I_n might occur, as an example, on proteins composed by heavier monomers exhibiting two or more thermodynamic domains, with the association core's domains remaining unaffected by the conformational change (that hence could be described as a modification involving the most "external" protein domains). Consequently, the dissociation phenomenon might occur concomitantly to the denaturation of the association core, for instance by following a scheme similar to the one of the first model her presented (Eq. (6)).

Therefore, such a scenario needs to consider two distinct equilibria, namely a one-step conformational transition equilibrium prior the concomitant dissociation/denaturation one, according to the following scheme

$$N_n \overset{K_I}{\leftrightarrow} I_n \overset{K}{\leftrightarrow} nD \tag{35}$$

being K_I and K the thermodynamic equilibrium constants related to the specific step and given by

$$K_I \equiv \frac{a_{I_n}}{a_{N_n}} \approx \frac{[I_n]}{[N_n]}\ \text{and}\ K \equiv \frac{a_D^n}{a_{I_n}} \approx \frac{[D]^n}{[I_n]} \tag{36}$$

considering that, for properly diluted solutions, the molar concentrations $[N_n]$, $[I_n]$, and $[D]$ are allowed to replace the thermodynamic activities a_{N_n}, a_{I_n}, and a_D, respectively.

By representing all the species in terms of monomers, the equilibria considered in Eq. (35) involve:

- "*NAM*" as the native monomer associated into the multimeric form $N_n$to be considered as the reference state;
- "*IAM*" as the intermediate monomer associated into the multimeric form I_n;
- "*D*" as the dissociated/denatured monomer.

According to the species listed above, the mass balance equation can be written as

$$[M]_{tot} = [NAM] + [IAM] + [D] \tag{37}$$

therefore, the partition function Q that considers the "*NAM*" state of the protein as reference becomes

$$Q = 1 + \frac{[IAM]}{[NAM]} + \frac{[D]}{[NAM]} \tag{38}$$

according to Eq. (3).

Accordingly, the monomer fraction present in the associated native state, f_{NAM}, the one present in the associated intermediate state, f_{IAM}, and the one present in the dissociated/denatured state, f_D, at a given temperature can be written as

$$f_{NAM} = \frac{1}{Q},\ f_{IAM} = \frac{[IAM]/[NAM]}{Q},\ \text{and}\ f_D = \frac{[D]/[NAM]}{Q},\ \text{with}\ f_{NAM} + f_{IAM} + f_D = 1 \tag{39}$$

Therefore, the overall enthalpy variation $\Delta H(T)$ of the whole process with respect to the reference state, *i.e.*, "*NAM*", becomes

$$\Delta H(T) = f_{IAM}\cdot\Delta_I H^\circ + f_D\cdot(\Delta_I H^\circ + \Delta_{dd}H^\circ) \tag{40}$$

being $\Delta_I H^\circ$ the standard enthalpy variation associated to the conformational transition leading to the formation of the intermediate "*IAM*" from the native "*NAM*" state, and $\Delta_{dd}H^\circ$ the standard enthalpy variation associated to the transition (dissociation/denaturation) from the "*IAM*" state to the "*D*" state. All these enthalpy variations are expressed per mole of the total monomers.

The temperature-derivative of $\Delta H(T)$ provides the theoretical specific heat capacity $C_p(T)$ curve that can be used to fit the experimental data. Hence, by following the same strategy described above to make the temperature-dependence of the $[IAM]/[NAM]$ and $[D]/[NAM]$ ratios explicit in terms of the model's fitting parameters, we obtain through Eqs. (36)–38

$$Q = 1 + K_I + \frac{K_I\cdot K}{n[D]^{n-1}} \tag{41}$$

whereas the respective f_{NAM}, f_{IAM}, and f_D fractions become

$$f_{NAM} = \frac{1}{Q},\ f_{IAM} = \frac{K_I}{Q},\ \text{and}\ f_D = \frac{K_I\cdot K}{n[D]^{n-1}}\frac{1}{Q} \tag{42}$$

where $[D]$ is obtainable from the resolution of the related mass balance equation (see Appendix D for details):

$$\frac{n(1+K_I)}{K_I K}[D]^n + [D] - n[N_n]_{tot} = 0 \tag{43}$$

Also in this case, the temperature dependence of both the equilibrium constants is obtainable by the solution of the van't Hoff equation. In particular, for the first step of conformational transition we have $K_I(T)$ that recalls the dependence of a thermodynamic constant for a denaturation phenomenon as in Eq. (31), *i.e.*,

$$K_I(T) = \exp\left[\frac{\Delta_I H^\circ}{R}\left(\frac{1}{T_I} - \frac{1}{T}\right)\right] \tag{44}$$

with T_I having the same meaning of that for a one-step conformational transition (that means $K_I(T_I) = 1$ as for Eq. (31)) and $\Delta_I H^\circ$ expressed per mole of monomer, whilst for the second equilibrium related to the dissociation/denaturation event, $K(T)$ is given by Eq. (15), with the

dissociation temperature, T_{diss}, defined as the temperature at which half of the multimer population in all possible states has undergone dissociation/denaturation (that means that $[N_n] + [I_n] = [N_n]_{tot}/2$ at this temperature), ΔH^{vH} considered as the enthalpy variation involved in the dissociation/denaturation step expressed per mole of multimer I_n, and $K(T_{diss})$ obtainable from the mass balance equation as reported in Appendix A.iii:

$$K(T_{diss}) = \frac{n^n [N_n]_{tot}^{n-1}}{2^{n-1}} \cdot \frac{1 + K_I(T_{diss})}{K_I(T_{diss})} \tag{45}$$

Also here, different sets of equations can be developed for the specific dissociation stoichiometries n of interest, thus achieving the theoretical specific heat capacity $C_p(T)$ curves given by the Eq. (5) and needed for DSC trace fit attempts. The fitting parameters characterizing this specific model are four (two for each equilibrium), namely T_I, $\Delta_I H^\circ$, T_{diss}, and ΔH^{vH}, being $\Delta_{dd} H^\circ = \Delta H^{vH}/n$.

The final equations for the model considering N_2, N_3, and N_4 proteins are shown explicitly in Appendix D and can be used to obtain the theoretical specific heat capacity $C_p(T)$ curve for each case, so to be applied for the fitting of the DSC thermograms.

In analogy with the models described above, we may note that the dependence of the equations on $[N_n]_{tot}$ is only apparent since this parameter is actually deleted through the substitution of the solutions to the overall equations that lead to the f_{NAM}, f_{IAM}, and f_D fractions as shown in Appendix D, as expected for equilibrium processes.

As an example, the final equations for $n = 2$ are listed below (see Appendix D for details):

$$Q = 1 + K_I + \frac{1}{2D'} \tag{46}$$

$$\text{with } D' = \frac{-1+\sqrt{1+8\frac{1+K_I}{K_I K^\circ}}}{4(1+K_I)} \text{ and } K^\circ_{diss} = \frac{1+K_I(T_{diss})}{K_I(T_{diss})} \cdot \exp\left[\frac{\Delta H^{vH}}{R}\left(\frac{1}{T_{diss}} - \frac{1}{T}\right)\right]$$

$$f_{NAM} = \frac{1}{Q},\ f_{IAM} = \frac{K_I}{Q},\ \text{and } f_D = \frac{1}{2D'Q} \tag{47}$$

$$C_p(T) = \frac{d\Delta H(T)}{dT},\ \text{with } \Delta H(T) = f_{IAM} \cdot \Delta_I H^\circ + f_D \cdot (\Delta_I H^\circ + \Delta_{dd} H^\circ) \text{ and } \Delta_{dd} H^\circ = \frac{\Delta H^{vH}}{2} \tag{48}$$

where T_I, $\Delta_I H^\circ$, T_{diss}, and ΔH^{vH} are the fitting parameters.

3. Results and applications

The most common scenario that includes dissociation is described by the first model (Eq. (6))

$$N_n \overset{K}{\leftrightarrow} nD$$

hence an equilibrium that reflects an always concomitant dissociation/denaturation of the multimeric protein.

In this case, the main characteristic of a DSC thermogram that should induce the suspect of the occurrence of a dissociation process is an asymmetry with respect to the T_{max}, with a prolonged part at lower temperatures and a steep descent of the trace followed by a gradual return to baseline at higher temperatures (Fig. 1).

Following the Occam's Razor philosophy, the fitting attempt on such a type of thermograms by using the simplest $N \leftrightarrow D$ thermodynamic model for a single-domain monomeric protein often fails, especially on the left hand of the profile since the equations produced through this model are symmetric [26,27]. Nonetheless, it is worth noting that single-domain monomeric proteins may sometimes show skewed denaturation peaks too if irreversible kinetic events occur simultaneously, such as post-denaturation protein aggregation phenomena [27]. However, although post-denaturation aggregation (even without a detectable exothermic contribution) can produce a depletion of the high-temperature region of the thermogram together with an abrupt signal drop (with a slope that usually is higher than the dissociation case [32]), the first part of the trace still reflects the first region of the symmetric profile typical of a simple protein native-to-denatured state equilibrium. In any case, kinetic phenomena can be previously recognized since they are sensitive to the DSC scanning rate as well as the overall protein concentration [33].

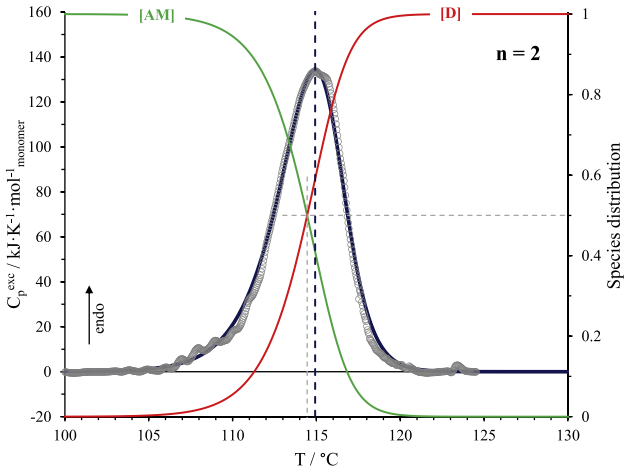

Fig. 1. *DSC thermal denaturation curve of TmArgBP reported from [32] (grey circles) and theoretical $C_p(T)$ trace (blue solid line) for $N_2 \leftrightarrow 2D$ equilibrium obtained by the application of Eqs. (17)–19. The distribution AM and D species are also shown by referring to the secondary axis.*

Furthermore, even the introduction of multiple thermodynamic domains produces an unsuccessful fit though usually asymmetric as well. Indeed, each domain curve involved results too broad (due to the splitting of the enthalpy values) to be compatible with a typical dissociation profile [14]. For the same reason, applying a dissociation scenario with $n \geq 2$ to model a DSC trace of a monomeric protein constituted by multiple thermodynamic domains produces an unsuccessful fit since, in this case, the enthalpy value per monomer required to reach the experimental profile produces a too sharp trace with respect to the experimental one.

As an example, Fig. 1 shows the DSC thermogram for an arginine-binding protein from *Thermotoga maritima* (TmArgBP), a system that was characterized on a previous work [32] and was found to exist as a high stability dimer at those experimental conditions, according to the test equations developed by Privalov and Potekhin [25]. As indicated above, the calorimetric signal exhibited by TmArgBP is asymmetric and shows a drop of the trace at higher temperatures. The application of Eqs. (17)–19, that are produced by considering a $N_2 \leftrightarrow 2D$ equilibrium, allows to achieve a satisfactory fit with $T_{diss} = 114.45$ °C and $\Delta H^{vH} = 1400$ kJ·mol^{-1} of N_2 (hence, $\Delta_{dd} H^\circ = 700$ kJ·mol^{-1} of monomer). Fig. 1 also shows the distribution of the species all considered as monomers, *i.e.*, *AM* defined as the monomer associated into the dimeric form and *D* defined as the monomer in its denatured state. It is possible to observe that the intersection of the two distribution curves, that of course occurs at a species distribution of 50 % for both, has an abscissa that corresponds to T_{diss} value, that is always lower than the T_{max} detected on an experimental DSC profile.

Focusing on the model under discussion (Eq. (6)), Fig. 2 shows the influence of n (dissociation stoichiometry), T_{diss}, and $\Delta_{dd} H^\circ$ (the latter being directly comparable to the experimental ΔH_{exp} value and corresponding to $\Delta_{dd} H^\circ = \Delta H^{vH}/n$) on the $C_p(T)$ profiles to emphasise the weight of each fitting parameter.

In particular, as concerns the influence of n by keeping T_{diss} and $\Delta_{dd} H^\circ$ constant (Fig. 2a), we observe that the left side of the thermogram is only slightly affected by the variation of n, whereas the trace drop on

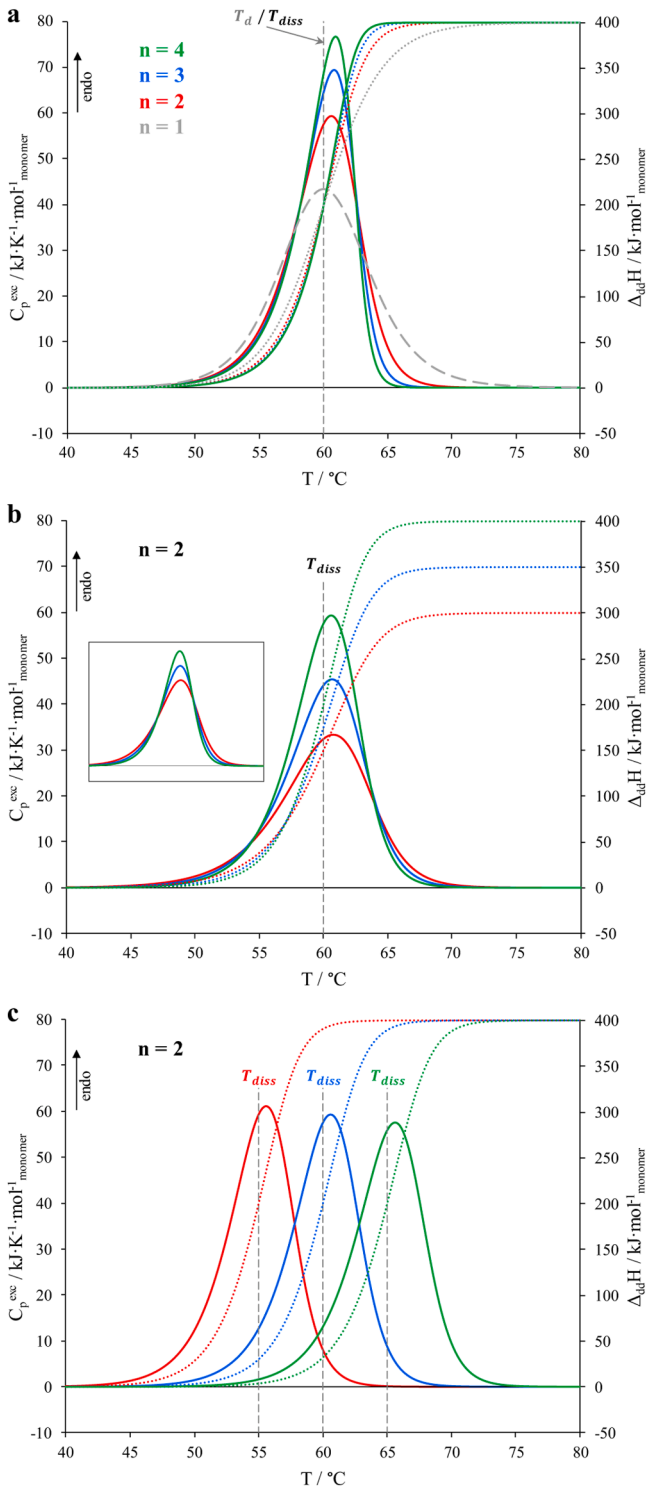

Fig. 2. Theoretical $C_p(T)$ profiles expressed per mole of protein monomers and comparing the influence of each single fitting parameters: a) comparison of various n by keeping $\Delta_{dd}H°$ and T_{diss} constant; b) comparison of various $\Delta_{dd}H°$ by keeping n and T_{diss} constant (for completeness, the inset also compares the peaks' contours at a common unitary enthalpy); c) comparison of various T_{diss} by keeping n and $\Delta_{dd}H°$ constant.

the right side becomes increasingly sharper as the value for n increases, as well as the peak height raises. This greater evidence of differences on the left side of the thermogram is to be found on the temperature dependence of K_{diss}. Indeed, at a certain ΔH^{vH}, K_{diss} depends more severely on temperature at higher temperatures just by the exponential itself, according to Eq. (15). Consequently, considering that ΔH^{vH} needs to become greater with the increase of n if we want to maintain the same $\Delta_{dd}H°$ ($\Delta H^{vH} = \Delta_{dd}H°{\cdot}n$), K_{diss} acquires a greater temperature dependence that becomes even much more relevant at higher temperatures with the increase of n.

Almost the same effect is also observed when varying the $\Delta_{dd}H°$ by keeping n and T_{diss} constant (Fig. 2b). Indeed, here ΔH^{vH} increases proportionally to $\Delta_{dd}H°$, and we observe a contraction of the peak at both its ends as expected for a $\Delta_{dd}H°$ increase, though the thermogram still results increasingly sharper on the right side for the same reason illustrated for the variation of n.

Instead, the variation of T_{diss}, by keeping n and $\Delta_{dd}H°$ constant, modifies the transition temperature region of course, but its influence on the profile results to be modest and only related to a slight reduction of the peak height with greater T_{diss} values.

At last, beside this inspection, it is important to emphasise that the risk of degeneracy for this model is rather low since this type of interrelation among the fitting parameters reduces the degrees of freedom and always produces a typical profile that, in general, is not able to fit an experimental profile that does not correspond to the simple model of concomitant dissociation/denaturation.

In the case the simplest dissociation model in Eq. (6) failed in fitting the experimental data, the application of the following models may also be attempted:

$$N_n \overset{K_{diss}}{\leftrightarrow} nM \overset{K_d}{\leftrightarrow} nD$$

$$N_n \overset{K_I}{\leftrightarrow} I_n \overset{K}{\leftrightarrow} nD$$

In both these cases, multiple equilibria are considered, hence, the number of fitting parameters rises to four for any stoichiometry chosen for the dissociation step, thus increasing the risk of degeneracy. Nonetheless, since these models are sequential, the position of the dissociation step produces scenarios that are fundamentally different, as shown in Fig. 3.

Going into details about the second model, which is characterized by a dissociation equilibrium followed by a denaturation step as represented by Eq. (20), a typical and reasonable theoretical profile is depicted in Fig. 4.

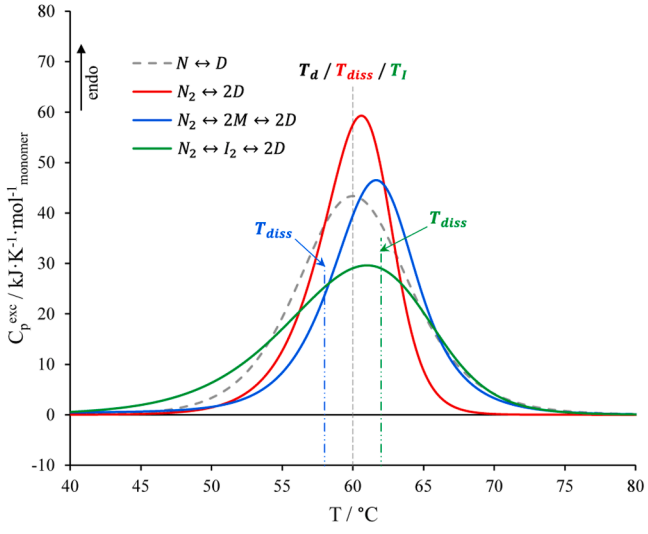

Fig. 3. Theoretical $C_p(T)$ traces produced through the three models (coloured solid traces) by involving the dissociation of a dimer N_2, also compared to the simplest N ↔ D profile (dashed grey trace) for completeness. For a fair comparison, the curves are presented with the same ΔH_{tot} of 400 kJ·mol^{-1} of monomer and with a common T_d (for both N ↔ D and N_2 ↔ 2M ↔ 2D models), T_{diss} (for the N_2 ↔ 2D model), and T_I (for the N_2 ↔ I_2 ↔ 2D model) corresponding to the value of 60 °C.

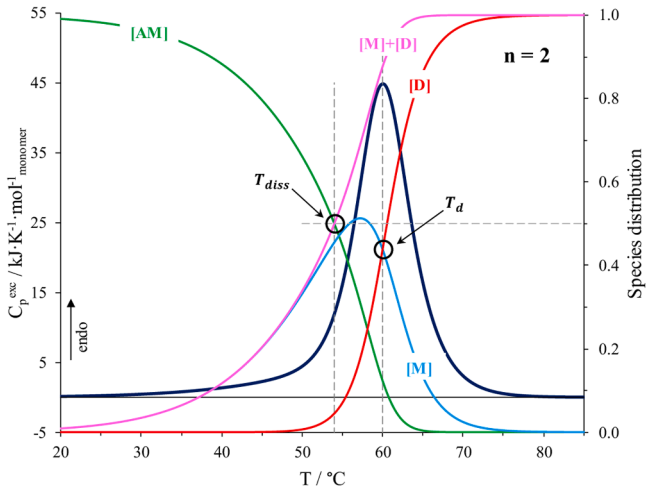

Fig. 4. Theoretical $C_p(T)$ trace (blue solid line) for $N_2 \leftrightarrow 2M \leftrightarrow 2D$ equilibria obtained by the application of Eqs. (32)–34. The parameter values used to obtain the curve are $T_{diss} = 54$ °C, $\Delta_{diss}H^\circ = 100$ kJ·mol^{-1} of monomer, $T_d = 60$ °C, and $\Delta_d H^\circ = 350$ kJ·mol^{-1} of monomer (hence, $\Delta H_{tot} = 450$ kJ·mol^{-1} of monomer). The distribution AM, M, and D species, together with $M+D$, are also shown by referring to the secondary axis.

In particular, we observe again an asymmetry of the curve characterized by an extended tail on the left side of the thermogram, that is dictated by the dissociation phenomenon, and a smoother signal drop on the right side of the thermogram, that recalls the typical symmetry of the trace describing the simplest one-step denaturation equilibrium. Logically, being $N_n \leftrightarrow nM \leftrightarrow nD$ constituted by two sequential equilibria each regulated by a couple of two fitting parameters, the profiles that can be provided by such a model are numerous. In any case, all of them have to be coherent with the scheme by basing on the same general assumption of considering a multimer with an association thermal stability that is lower than the overall thermal stability of the monomer form against denaturation, that means $T_{diss} < T_d$, as well as having a total enthalpy variation mainly given by the denaturation step, that means $\Delta_{diss}H^\circ < \Delta_d H^\circ$.

Furthermore, taking advantage of the species distribution curves reported in Fig. 4, two meaningful intersection points can also be observed, the first between the distributions of *AM* and $M+D$, the second between the distributions of *M* and *D*: the x-coordinate of two points corresponds to the T_{diss} and to the T_d, respectively. Specifically, it is worth to emphasise that the intersection giving T_{diss} always occurs when both *AM* and $M+D$ reach a molar fraction of 0.5, that reflects the definition of T_{diss} as temperature at which $[N_n] = [N_n]_{tot}/2$, whereas the intersection giving T_d always occurs when *M* and *D* reach a 1:1 molar ratio, according to common definition reported above.

To highlight the weight of the fitting parameters on the $C_p(T)$ pro-

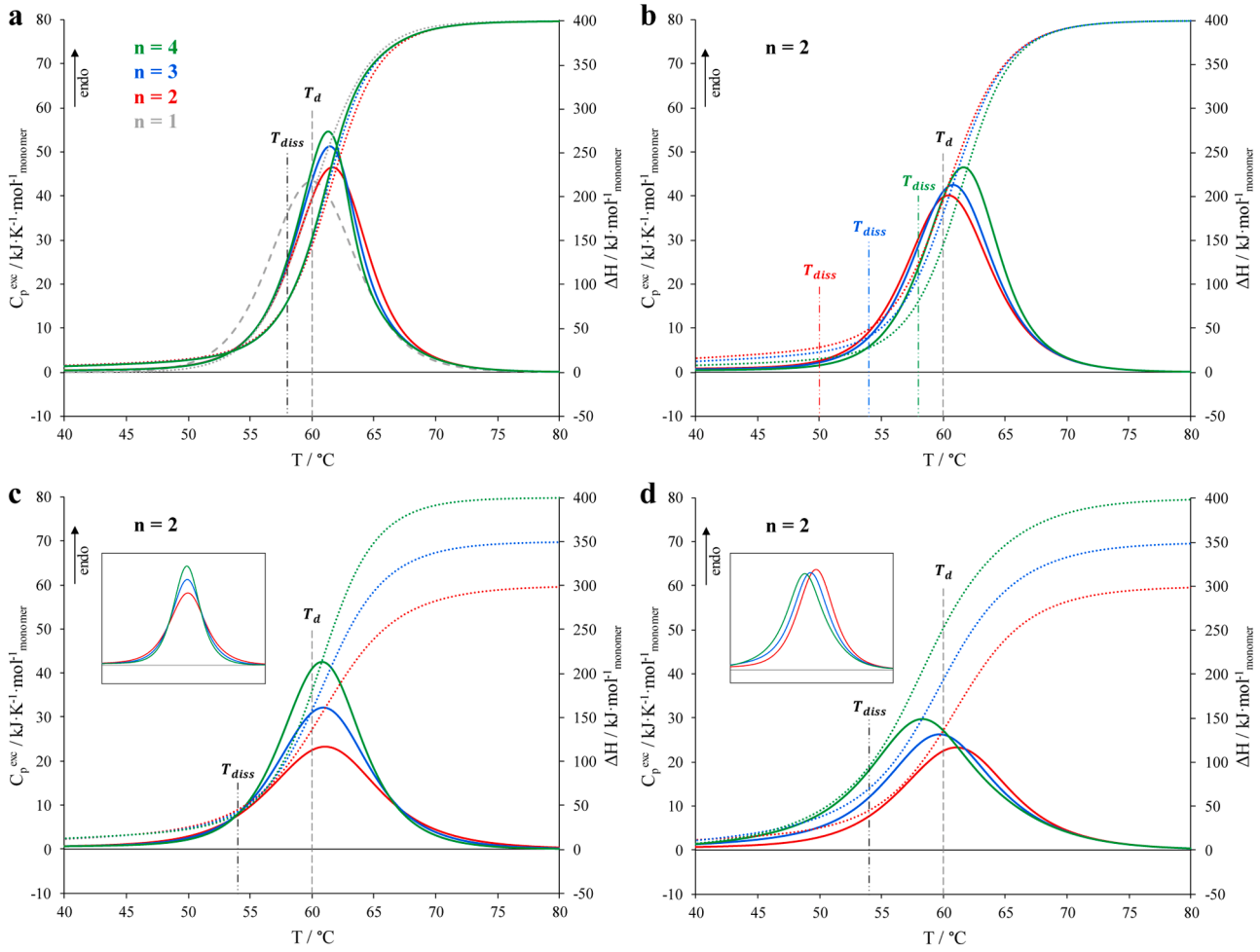

Fig. 5. Theoretical $C_p(T)$ profiles expressed per mole of protein monomers and comparing the influence of each single fitting parameters (T_d is always considered as a constant for simplicity): a) comparison of various *n* by keeping T_{diss}, $\Delta_d H^\circ$, and $\Delta_{diss}H^\circ$ constant; b) comparison of various T_{diss} by keeping *n*, $\Delta_d H^\circ$, and $\Delta_{diss}H^\circ$ constant; c) comparison of various $\Delta_d H^\circ$ by keeping *n*, T_{diss}, and $\Delta_{diss}H^\circ$ constant; d) comparison of various $\Delta_{diss}H^\circ$ by keeping *n*, T_{diss}, and $\Delta_d H$ constant. For completeness, the insets in panels c and d also compare the peaks' contours at a common unitary enthalpy.

files, the influence of n (dissociation stoichiometry), T_{diss}, $\Delta_d H^\circ$, and $\Delta_{diss} H^\circ$ (the latter being preferred instead of ΔH^{vH} for the comparison because $\Delta_{diss} H^\circ = \Delta H^{vH}/n$ and it is expressed per mole of monomer) are illustrated in Fig. 5.

As concerns the influence of n (Fig. 5a), analogously to the first model we observe that the peak height raises, and the profile becomes sharper on the right side as the value for n increases because of the dependence of $K_{diss}(T)$ on ΔH^{vH} (see above). Nonetheless, the very last part of the peak ends smoothly and similarly regardless n since the main contribution is given by the denaturation event, whilst the K_{diss} does not affect this region significantly.

When inspecting the effect of the gap between the two temperature parameters, that in fact consists in outdistancing the two equilibria, Fig. 5b reveals that the profile becomes slightly broader and gains symmetry as the distance between the two events increases. Actually, this behaviour is unsurprising because the greater the gap between T_{diss} and T_d, the less the peak contributions separately ascribable to dissociation and denaturation overlap to each other, hence leading to a profile almost symmetric if not for its very beginning.

At last, as regards the effects of the enthalpic contributions, Fig. 5c shows that the increase of the $\Delta_d H^\circ$ term causes the growth of the peak height together with a slight contraction of the peak at both its ends, though a bit greater on the right side of the tracing, as expected for a common one-step protein denaturation profile and emphasised by the figure's inset comparing curves normalized at unitary areas. On the other hand, the increment of $\Delta_{diss} H^\circ$ makes the dissociation event more significant when summing the two contributions to obtain the overall profile (Fig. 5d). Therefore, it results in an overall broadening of the $C_p(T)$ curve with a downshift of the peak maximum towards lower temperatures as the dissociation equilibrium becomes increasingly more enthalpically relevant.

Concerning the case of a more complex scenario (Eq. (35)), instead, the $N_n \leftrightarrow I_n \leftrightarrow nD$ model considers the possibility of a multimeric protein that undergoes a partial conformational transition with a consecutive dissociation/denaturation equilibrium. In particular, the first step conformational transition in the protein is assumed to not compromise the association region of the protein yet, which remains still resilient till the dissociation process occurs at higher temperature ($T_I < T_{diss}$). As mentioned above, this scenario is likely shown in some cases by heavier proteins that might exhibit multiple thermodynamic domains that behave differently. An example of theoretical curve produced by the application of the model under discussion is reported in Fig. 6.

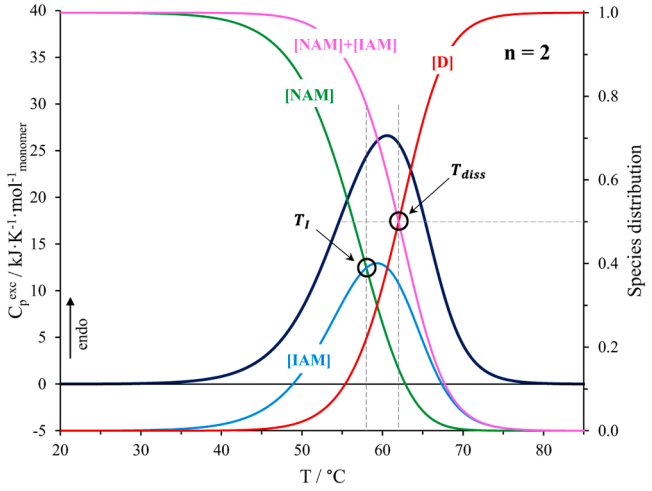

Fig. 6. Theoretical $C_p(T)$ trace (blue solid line) for $N_2 \leftrightarrow I_2 \leftrightarrow 2D$ equilibria obtained by the application of Eqs. (46)–48. The parameter values used to obtain the curve are $T_I = 58$ °C, $\Delta_I H^\circ = 200$ kJ·mol^{-1} of monomer, $T_{diss} = 62$ °C, and $\Delta_{dd} H^\circ = 200$ kJ·mol^{-1} of monomer (hence, $\Delta H_{tot} = 400$ kJ·mol^{-1} of monomer). The distribution NAM, IAM, and D species, together with NAM+IAM, are also shown by referring to the secondary axis.

Also in this case, we observe an asymmetric profile that usually covers larger temperature intervals because of a significantly extended low-temperature region followed by a signal drop that recalls the properties of the first model in Fig. 1.

Furthermore, Fig. 6 also reports the distribution curves for all the species involved in the process. Analogously to the second model, we can note two intersection points between *NAM* and *IAM* curves and between *NAM* + *IAM* and *D* curves, indicating T_I and T_{diss} on the x-axis, respectively. In particular, since the meaning of T_I is somehow related to the definition of T_d, it always occurs when *NAM* and *IAM* reach a 1:1 molar ratio, whilst the T_{diss} intersection always occurs when *NAM* + *IAM* and *D* achieve a molar fraction of 0.5, according to the definition reported above.

Following the same strategy applied so far, we also compared in Fig. 7 the effects of all the fitting parameters on the $C_p(T)$ curve generated by this third model.

As regards the influence of n (Fig. 7a), we observe profiles becoming increasingly sharper on the right side as the value for n increases, also producing a discreet upshift of the peak maximum towards higher temperatures as a consequence. Considering that n is a parameter involved in the dissociation process only, it can be reasonably noted that it affects only the second half region of the thermogram coherently to what exhibited by the first model in Fig. 2a, whilst the first part is completely unaffected.

When analysing the influence of outdistancing the two equilibria by increasing the gap between T_I and T_{diss} (Fig. 7b), we observe that the profiles become continuously broader and more asymmetric. Being both the two contributions underneath the overall $C_p(T)$ curve significant in terms of areas, peak shoulders may appear even if the two temperature parameters are not exaggeratedly far from each other.

At last, as regards the effects of the enthalpic contributions, Fig. 7c and d show variations on the peak outline according to the increase of either the $\Delta_I H^\circ$ or the $\Delta_{dd} H^\circ$, respectively. Specifically, the $\Delta_I H^\circ$ term only contributes to a peak area increase together with a slight downshift of the peak maximum towards lower temperatures, leaving the late part of the curve unaffected. On the other hand, the $\Delta_{dd} H^\circ$ terms leads to a sharper signal drop consequently to the right side's area increment, together with a discreet upshift of the peak maximum towards higher temperatures, as expected for a modification of ΔH^{vH} that directly influences the $K_{diss}(T)$ dependence. In this last case, the low-temperature region of the thermogram is also slightly affected, as emphasised by Fig. 7d's inset that only focuses on the thermogram contours by comparing traces with unitary areas.

Fig. 8 reports as an example the fitting attempts undertaken on the experimental DSC profile recorded for peanut agglutinin (PNA), a galactose-recognizing lectin from *Arachis hypogaea* studied for other aspects in a previous work [34].

PNA is reported in the literature to be a homotetramer, or, by being more precise, a dimer of dimers, with a very peculiar open quaternary structure characterized by only three inter-subunits interfaces at physiological pH [35].

For a protein with known multimeric structure, the asymmetry of the profile is itself a strong indication of the occurrence of a dissociation event, provided that no simpler model produces satisfactory fits (see above). The application of the first ($N_4 \leftrightarrow 4D$) and the second ($N_4 \leftrightarrow 4M \leftrightarrow 4D$) model were unable to give back reasonable fits whereas a fair fit was obtained for the scheme $N_4 \leftrightarrow I_4 \leftrightarrow 4D$ (third model with $T_I = 52.7$ °C, $\Delta_I H^\circ = 240$ kJ·mol^{-1} of monomer, $T_{diss} = 57.0$ °C, and $\Delta_{dd} H^\circ = 180$ kJ·mol^{-1} of monomer), confirming the above analysis for which, despite the presence of four fitting parameters, the probability of degeneracy between these sequential equilibrium models is very low.

A detailed analysis of this protein, reported here as an example, is beyond the scope of this paper. Nonetheless, for the sake of complete-

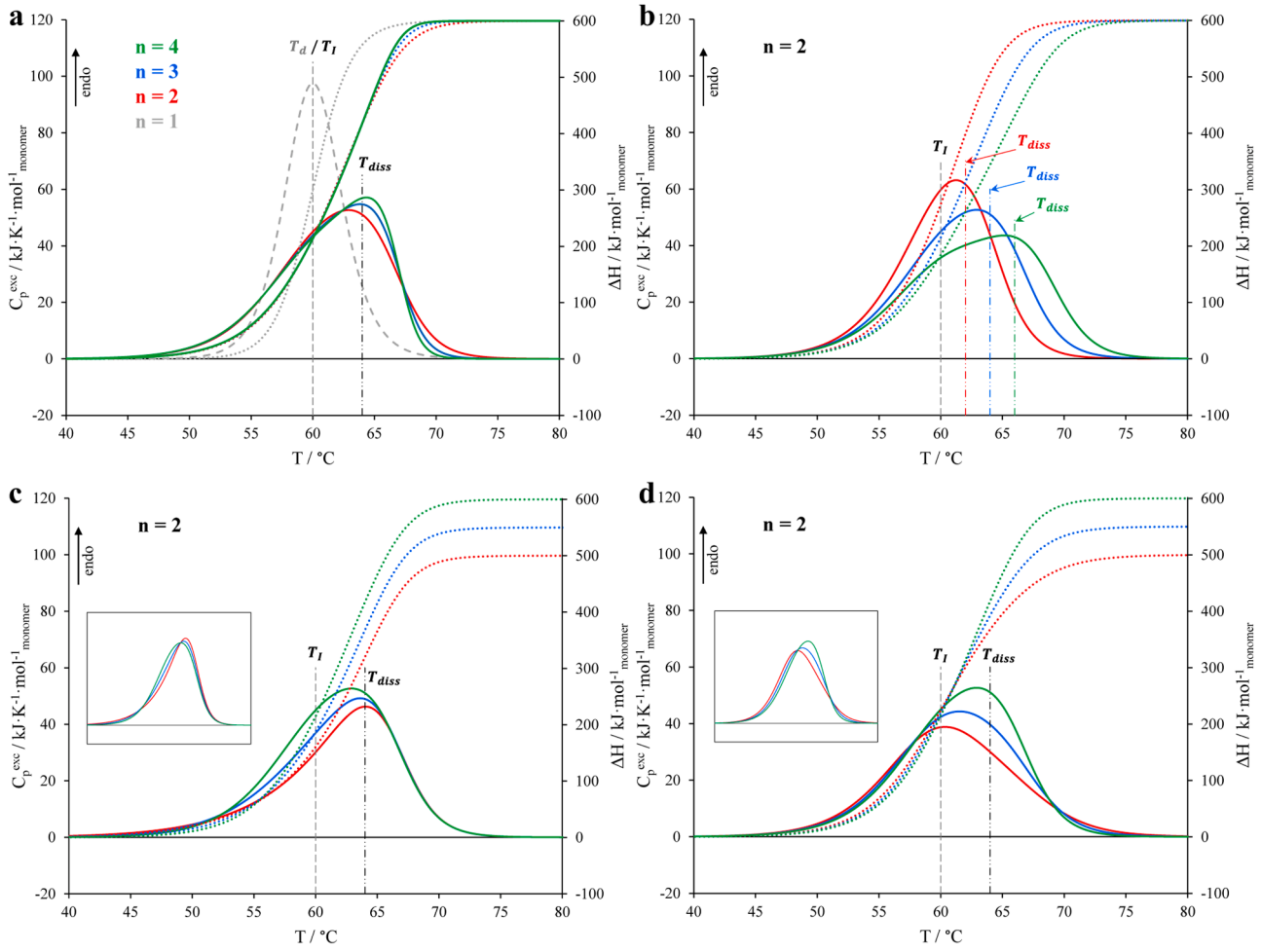

Fig. 7. Theoretical $C_p(T)$ profiles expressed per mole of protein monomers and comparing the influence of each single fitting parameters (T_I is always considered as a constant for simplicity): a) comparison of various n by keeping T_{diss}, $\Delta_I H^\circ$, and $\Delta_{dd}H^\circ$ constant; b) comparison of various T_{diss} by keeping n, $\Delta_I H^\circ$, and $\Delta_{dd}H^\circ$ constant; c) comparison of various $\Delta_I H^\circ$ by keeping n, T_{diss}, and $\Delta_{dd}H^\circ$ constant; d) comparison of various $\Delta_{dd}H^\circ$ by keeping n, T_{diss}, and $\Delta_I H^\circ$ constant. For completeness, the insets in panels c and d also compare the peaks' contours at a common unitary enthalpy.

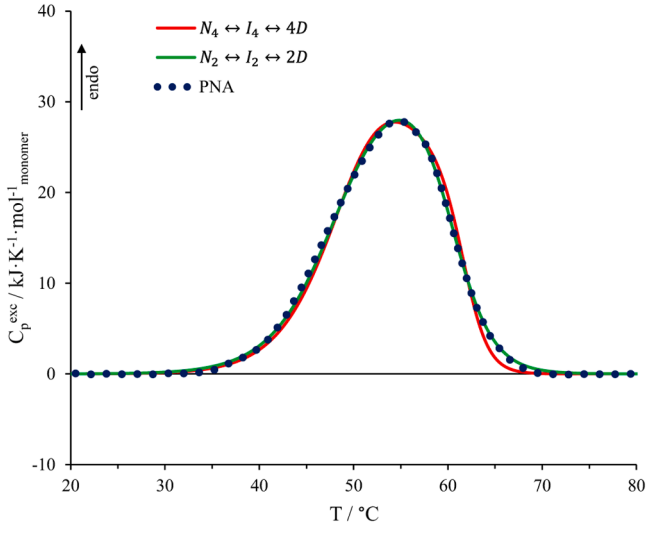

Fig. 8. DSC thermal denaturation curve of PNA reported from [34] (blue dots) and theoretical $C_p(T)$ traces for $N_4 \leftrightarrow I_4 \leftrightarrow 4D$ equilibria (red solid line) and $N_2 \leftrightarrow I_2 \leftrightarrow 2D$ equilibria (green solid line).

ness, we report here that an amelioration of the fit was obtained by considering the scheme $N_2 \leftrightarrow I_2 \leftrightarrow 2D$ (with $T_I = 51.5$ °C, $\Delta_I H^\circ = 220$ kJ·mol^{-1} of monomer, $T_{diss} = 56.8$ °C, and $\Delta_{dd}H^\circ = 210$ kJ·mol^{-1} of monomer), that is consistent with the idea of "dimer of dimers" supposing a prior low energetic dissociation event of the tetramer to dimers. However, the profile differences obtained by $n = 2$ or $n = 4$ are small and very close to the experimental error. This means that, despite the probability of degeneracy between these complex models is low, the risk of degeneracy within the same model as regards the stoichiometry exists, and further information might be needed (structural information, experiments at different conditions, *etc.*) to assess the real scenario.

4. Conclusions

This study shows the development and some applications of new stand-alone thermodynamic equations useful for the description of dissociation/denaturation phenomena from DSC thermograms, which usually display an asymmetry of the calorimetric trace in such cases. The three models proposed, which mainly differentiate from each other for the simultaneity or sequentiality with which protein dissociation and denaturation occur, highlight how the calorimetric profiles can be different according to the underlying dissociation/denaturation molecular mechanism. Consequentially, the risk of degeneracy between the three models during a fitting procedure is very low in fact. On the other hand, the risk of degeneracy might increase when trying to discriminate

among different dissociation stoichiometries (n parameter) within the same model, especially for models with more than two fitting parameters (as happens for the second and the third ones presented here).

In general, this study addresses a significant gap in the thermodynamic modelling of multimeric protein denaturation processes that involve dissociation events. Furthermore, this study also provides practical, ready-to-use solutions for the most common homomers (dimers, trimers, and tetramers), making these complex equations accessible for a better understanding of the conformational stability of multimeric proteins, which may have direct implications on biological and pharmaceutical (or similar) research fields.

The general methodology and strategy proposed for the development of these models, that link the statistical mechanics concept of partition function with the classical thermodynamics' equilibrium constant also for the multimeric proteins, pave the way for the development of models that may reflect more complex scenarios than those considered in this work, if the case.

CRediT authorship contribution statement

Dimitrios Fessas: Writing – review & editing, Writing – original draft, Validation, Methodology, Formal analysis, Data curation, Conceptualization. **Francesca Saitta:** Writing – review & editing, Writing – original draft, Visualization, Validation, Methodology, Formal analysis, Data curation.

Declaration of competing interest

The authors declare that they have no known competing financial interests or personal relationships that could have appeared to influence the work reported in this paper.

Appendix A

Determination of $K(T_{diss})$ for the three models

The term $K(T_{diss})$ is the value of the equilibrium constant at the dissociation temperature. T_{diss} is defined as the temperature at which $[N_n] = [N_n]_{tot}/2$ for the model *i)* and *ii)*, whereas $[N_n] + [I_n] = [N_n]_{tot}/2$ for the model *iii)*. In detail, the value for $K(T_{diss})$ can be obtained from the mass balance equation specific for each equilibrium considered and the from the corresponding relation for the equilibrium constant under the approximation of equality between the thermodynamic activities and the related molar concentration terms.

i) $N_n \overset{K}{\leftrightarrow} nD$

The mass balance equation for this equilibrium is

$$n[N_n]_{tot} = [AM] + [D] \tag{A.1}$$

$$n[N_n]_{tot} = n[N_n] + [D] \tag{A.2}$$

By substituting $[N_n]$ with the corresponding value at $T = T_{diss}$, we have

$$n[N_n]_{tot} = n\frac{[N_n]_{tot}}{2} + [D] \tag{A.3}$$

$$[D] = n\frac{[N_n]_{tot}}{2} \tag{A.4}$$

Therefore, the $K(T_{diss})$ can be written as

$$K(T_{diss}) = \frac{[D]^n}{[N_n]} = \left(\frac{n^n[N_n]^n_{tot}}{2^n}\right) \Big/ \left(\frac{[N_n]_{tot}}{2}\right) = \frac{n^n[N_n]^{n-1}_{tot}}{2^{n-1}} \tag{A.5}$$

For the sake of completeness, we report here the $K(T_{diss})$ values for the three most common n:

$$n = 2: \quad K(T_{diss}) = 2[N_2]_{tot}$$

$$n = 3: \quad K(T_{diss}) = 27/4[N_3]^2_{tot}$$

$$n = 4: \quad K(T_{diss}) = 32[N_4]^3_{tot}$$

ii) $N_n \overset{K_{diss}}{\leftrightarrow} nM \overset{K_d}{\leftrightarrow} nD$

The mass balance equation for this equilibrium is

$$n[N_n]_{tot} = [AM] + [M] + [D] \tag{A.6}$$

$$n[N_n]_{tot} = n[N_n] + [M] + K_d[M] \tag{A.7}$$

$$n[N_n]_{tot} = n[N_n] + [M](1 + K_d) \tag{A.8}$$

By substituting $[N_n]$ with the corresponding value at $T = T_{diss}$, we have

$$[M] = n\frac{[N_n]_{tot}}{2}\frac{1}{1 + K_d(T_{diss})} \tag{A.9}$$

with $K_d(T_{diss})$ being the value of the monomer denaturation constant at the dissociation temperature T_{diss}.

Consequently, the $K_{diss}(T_{diss})$ can be written as

$$K_{diss}(T_{diss}) = \frac{[M]^n}{[N_n]} = \left\{\frac{n^n[N_n]_{tot}^n}{2^n[1+K_d(T_{diss})]^n}\right\} \Big/ \left(\frac{[N_n]_{tot}}{2}\right) = \frac{n^n[N_n]_{tot}^{n-1}}{2^{n-1}} \cdot \frac{1}{[1+K_d(T_{diss})]^n} \tag{A.10}$$

For the sake of completeness, we report here the $K_{diss}(T_{diss})$ values for the three most common n:

$$n=2: \; K_{diss}(T_{diss}) = 2[N_2]_{tot} \frac{1}{[1+K_d(T_{diss})]^2}$$

$$n=3: \; K_{diss}(T_{diss}) = 27/4[N_3]_{tot}^2 \frac{1}{[1+K_d(T_{diss})]^3}$$

$$n=4: \; K_{diss}(T_{diss}) = 32[N_4]_{tot}^3 \frac{1}{[1+K_d(T_{diss})]^4}$$

with $K_d(T_{diss}) = \exp\left[\frac{\Delta_d H^\circ}{R}\left(\frac{1}{T_d} - \frac{1}{T_{diss}}\right)\right]$.

iii) $N_n \overset{K_I}{\leftrightarrow} I_n \overset{K}{\leftrightarrow} nD$

The mass balance equation for this equilibrium is

$$n[N_n]_{tot} = [NAM] + [IAM] + [D] \tag{A.11}$$

$$n[N_n]_{tot} = n([N_n] + [I_n]) + [D] \tag{A.12}$$

By substituting $[N_n] + [I_n]$ with the corresponding value at $T = T_{diss}$, *i.e.*,

$$[N_n] + [I_n] = [N_n]_{tot}/2 \tag{A.13}$$

we have

$$[D] = n\frac{[N_n]_{tot}}{2} \tag{A.14}$$

Therefore, the $K(T_{diss})$ can be written as

$$K(T_{diss}) = \frac{[D]^n}{[I_n]} = \left(\frac{n^n[N_n]_{tot}^n}{2^n}\right) \Big/ \left(\frac{[N_n]_{tot}}{2} \cdot \frac{K_I(T_{diss})}{1+K_I(T_{diss})}\right) = \frac{n^n[N_n]_{tot}^{n-1}}{2^{n-1}} \cdot \frac{1+K_I(T_{diss})}{K_I(T_{diss})} \tag{A.15}$$

by considering the definition of K_I (Eq. (36) and Eq. (A.13)).

For the sake of completeness, we report here the $K(T_{diss})$ values for the three most common n:

$$n=2: \; K(T_{diss}) = 2[N_2]_{tot} \frac{1+K_I(T_{diss})}{K_I(T_{diss})}$$

$$n=3: \; K(T_{diss}) = 27/4[N_3]_{tot}^2 \frac{1+K_I(T_{diss})}{K_I(T_{diss})}$$

$$n=4: \; K(T_{diss}) = 32[N_4]_{tot}^3 \frac{1+K_I(T_{diss})}{K_I(T_{diss})}$$

with $K_I(T_{diss}) = \exp\left[\frac{\Delta_I H^\circ}{R}\left(\frac{1}{T_I} - \frac{1}{T_{diss}}\right)\right]$.

Appendix B

Derivation of equations for the $N_n \leftrightarrow nD$ model

Let's consider that, to obtain the $C_p(T)$ curve, it is necessary to know the distribution of all the fractions of protein f_i involved in the process, for which the knowledge of the partition function Q is always needed. This means that the derivation of the equations for every model below is driven by the need of making the partition function Q explicit in terms of the lowest number possible of fitting parameters.

i) $N_2 \overset{K}{\leftrightarrow} 2D$

The partition function Q is given by Eq. (12) and becomes for $n = 2$

$$Q = 1 + \frac{K}{2[D]} \tag{B.1}$$

The $[D]$ term can be determined by merging the mass balance equation (Eq. (A.2)) and the corresponding relation for the equilibrium constant under the approximation of equality between the thermodynamic activities and the related molar concentration terms (Eq. (7))

$$n[N_n]_{tot} = \frac{n}{K}[D]^n + [D] \tag{B.2}$$

$$\frac{n}{K}[D]^n + [D] - n[N_n]_{tot} = 0 \tag{B.3}$$

that becomes for $n = 2$

$$\frac{2}{K}[D]^2 + [D] - 2[N_2]_{tot} = 0 \tag{B.4}$$

with

$$[D] = \frac{-1 + \sqrt{1 + 16\frac{[N_2]_{tot}}{K}}}{4} \cdot K \tag{B.5}$$

The term K is dependent on temperature according to the van't Hoff equation

$$K(T) = K(T_{diss}) \cdot \exp\left[\frac{\Delta H^{vH}}{R}\left(\frac{1}{T_{diss}} - \frac{1}{T}\right)\right] = K(T_{diss}) \cdot K' = 2[N_2]_{tot} \cdot K' \tag{B.6}$$

where $K(T_{diss})$ is substituted according to Eq. (A.5) for $n = 2$, and K' is defined as the exponential term of Eq. (B.6).

By replacing K in Eq. (B.5) with Eq. (B.6), we obtain

$$[D] = \frac{-1 + \sqrt{1 + \frac{8}{K'}}}{4} \cdot K \tag{B.7}$$

and, by gathering the $\left(-1 + \sqrt{1 + 8/K'}\right)/4$ fraction under the symbol D',

$$[D] = D' \cdot K \tag{B.8}$$

Therefore, the partition function Q from Eq. (B.1) becomes

$$Q = 1 + \frac{2[N_2]_{tot} \cdot K'}{4D'[N_2]_{tot} \cdot K'} = 1 + \frac{1}{2D'} \tag{B.9}$$

noting that the $[N_2]_{tot}$ terms are mutually deleted, whereas the population fractions f_{AM} and f_D are obtained as

$$f_{AM} = \frac{1}{Q} \text{ and } f_D = \frac{1}{2D'Q} \tag{B.10}$$

and the temperature-dependent enthalpy variation involved in the process, expressed per mole of monomer, is obtained as

$$\Delta H(T) = f_D \cdot \Delta_{dd}H^{\circ} \text{ with } \Delta_{dd}H^{\circ} = \frac{\Delta H^{vH}}{2} \tag{B.11}$$

For this specific model, T_{diss} and ΔH^{vH} are the only fitting parameters gathered under the D' term, and there is no dependence on protein concentration (please note that each grouping under symbols, namely K' and D', is free from the total protein concentration term).

ii) $N_3 \overset{K}{\leftrightarrow} 3D$

The partition function Q is given by Eq. (12) and becomes for $n = 3$

$$Q = 1 + \frac{K}{3[D]^2} \tag{B.12}$$

The $[D]$ term can be determined by merging the mass balance equation (Eqs. (A.2) and (B.3)) and the corresponding relation for the equilibrium constant under the approximation of equality between the thermodynamic activities and the related molar concentration terms (Eq. (7)). For $n = 3$, Eq. (B.3) becomes

$$\frac{3}{K}[D]^3 + [D] - 3[N_3]_{tot} = 0 \tag{B.13}$$

Being Eq. (B.13) a third-order equation, we can consider that the analytical solution for the generic $ax^3 + bx^2 + cx + d = 0$ $(a \neq 0)$ is given by

$$x = -\frac{b}{3a} + \sqrt[3]{-\frac{q}{2} + \sqrt{\Delta}} + \sqrt[3]{-\frac{q}{2} - \sqrt{\Delta}} \tag{B.14}$$

when $\Delta > 0$, with

$$p = \frac{c}{a} - \frac{b^2}{3a^2} \tag{B.15}$$

$$q = \frac{d}{a} - \frac{bc}{3a^2} + \frac{2b^3}{27a^3} \tag{B.16}$$

$$\Delta = \frac{q^2}{4} + \frac{p^3}{27} \tag{B.17}$$

For Eq. (B.13), the p, q and, $\sqrt{\Delta}$ terms (the latter directly considered as square root for convenience) can be written as

$$p = \frac{K}{3} \tag{B.18}$$

$$q = -[N_3]_{tot}K \tag{B.19}$$

$$\sqrt{\Delta} = K\sqrt{\frac{[N_3]_{tot}^2}{4} + \frac{K}{27^2}} \tag{B.20}$$

Considering that K depends on temperature according to

$$K(T) = K(T_{diss})\cdot\exp\left[\frac{\Delta H^{vH}}{R}\left(\frac{1}{T_{diss}} - \frac{1}{T}\right)\right] = K(T_{diss})\cdot K' = \frac{27}{4}[N_3]_{tot}^2\cdot K' \tag{B.21}$$

where $K(T_{diss})$ is substituted according to Eq. (A.5) for $n = 3$, and K' is defined as the exponential term of Eq. (B.21), for the sake of simplicity, Eq. (B.20) can be further simplified by including Eq. (B.21):

$$\sqrt{\Delta} = K\sqrt{\frac{[N_3]_{tot}^2}{4} + \frac{[N_3]_{tot}^2\cdot K'}{27\cdot 4}} = \frac{[N_3]_{tot}K}{2}\sqrt{1 + \frac{K'}{27}} = \frac{[N_3]_{tot}K}{2}\sqrt{\Delta'} \tag{B.22}$$

with Δ' indicating the radicand for simplicity.

Therefore, the analytical solution for Eq. (B.13) is

$$[D] = x = \sqrt[3]{\frac{[N_3]_{tot}K}{2} + \frac{[N_3]_{tot}K}{2}\sqrt{\Delta'}} + \sqrt[3]{\frac{[N_3]_{tot}K}{2} - \frac{[N_3]_{tot}K}{2}\sqrt{\Delta'}} = \sqrt[3]{\frac{[N_3]_{tot}K}{2}(1 + \sqrt{\Delta'})} + \sqrt[3]{\frac{[N_3]_{tot}K}{2}(1 - \sqrt{\Delta'})} \tag{B.23}$$

By including Eq. (B.21), we have

$$[D] = \sqrt[3]{\frac{3^3[N_3]_{tot}^3K'}{2^3}(1 + \sqrt{\Delta'})} + \sqrt[3]{\frac{3^3[N_3]_{tot}^3K'}{2^3}(1 - \sqrt{\Delta'})} = \frac{3[N_3]_{tot}}{2}\left[\sqrt[3]{K'(1 + \sqrt{\Delta'})} + \sqrt[3]{K'(1 - \sqrt{\Delta'})}\right] = \frac{3[N_3]_{tot}}{2}\cdot D' \tag{B.24}$$

where D' indicates the contents enclosed by brackets.

At last, by replacing K and $[D]$ according to Eqs. (B.21) and (B.24), respectively, the partition function Q in Eq. (B.12) becomes

$$Q = 1 + \frac{K'}{(D')^2} \tag{B.25}$$

noting that the $[N_3]_{tot}$ terms are mutually deleted, whereas the population fractions f_{AM} and f_D are obtained as

$$f_{AM} = \frac{1}{Q} \text{ and } f_D = \frac{K'}{(D')^2 Q} \tag{B.26}$$

and the temperature-dependent enthalpy variation involved in the process, expressed per mole of monomer, is obtained as

$$\Delta H(T) = f_D\cdot\Delta_{dd}H^{\circ} \text{ with } \Delta_{dd}H^{\circ} = \frac{\Delta H^{vH}}{3} \tag{B.27}$$

For this specific model, T_{diss} and ΔH^{vH} are the only fitting parameters gathered under the D' term, and there is no dependence on protein concentration (please note that each grouping under symbols, namely K' and D', is free from the total protein concentration term).

iii) $N_4 \overset{K}{\leftrightarrow} 4D$

The partition function Q is given by Eq. (12) and becomes for $n = 4$

$$Q = 1 + \frac{K}{4[D]^3} \tag{B.28}$$

The $[D]$ term can be determined by merging the mass balance equation and the corresponding relation for the equilibrium constant under the approximation of equality between the thermodynamic activities and the related molar concentration terms, that finally provides Eq. (B.3). For $n = 4$, Eq. (B.3) becomes

$$\frac{4}{K}[D]^4 + [D] - 4[N_4]_{tot} = 0 \tag{B.29}$$

Eq. (B.29) is a fourth-order equation, thus, among the four solutions available, we can consider that the only valid analytical solution for the generic $ax^4 + bx^3 + cx^2 + dx + e = 0$ $(a \neq 0)$ is given by

$$x = -\frac{b}{4a} - Z + \frac{1}{2}\sqrt{-4Z^2 - 2p + \frac{S}{Z}} \tag{B.30}$$

where

$$p = \frac{8ac - 3b^2}{8a^2} \tag{B.31}$$

$$S = \frac{8a^2d - 4abc + b^3}{8a^3} \tag{B.32}$$

$$Z = \frac{1}{2}\sqrt{-\frac{2}{3}p + \frac{1}{3a}\left(\Delta_0 + \frac{q}{\Delta_0}\right)} \tag{B.33}$$

with

$$\Delta_0 = \sqrt[3]{\frac{s + \sqrt{s^2 - 4q^3}}{2}} \tag{B.34}$$

$$q = 12ae - 3bd + c^2 \tag{B.35}$$

$$s = 27ad^2 - 72ace + 27b^2e - 9bcd + 2c^3 \tag{B.36}$$

Considering that K depends on temperature according to

$$K(T) = K(T_{diss})\cdot\exp\left[\frac{\Delta H^{vH}}{R}\left(\frac{1}{T_{diss}} - \frac{1}{T}\right)\right] = K(T_{diss})\cdot K' = 32[N_4]_{tot}^3\cdot K' \tag{B.37}$$

where $K(T_{diss})$ is substituted according to Eq. (A.5) for $n = 4$, and K' is defined as the exponential term of Eq. (B.37), for the sake of simplicity, all the terms from Eq. (B.31) to Eq. (B.36) can be calculated:

$$s = \frac{27}{8[N_4]_{tot}^3 K'} \tag{B.38}$$

$$q = -\frac{6}{[N_4]_{tot}^2 K'} \tag{B.39}$$

$$\Delta_0 = \sqrt[3]{\frac{1}{2}\left[\frac{27}{8[N_4]_{tot}^3 K'} + \sqrt{\left(\frac{27}{8[N_4]_{tot}^3 K'}\right)^2 + 4\left(\frac{6}{[N_4]_{tot}^2 K'}\right)^3}\right]} = \frac{1}{[N_4]_{tot}}\sqrt[3]{\frac{1}{2}\left[\frac{27}{8K'} + \frac{1}{K'}\sqrt{\left(\frac{27}{8}\right)^2 + \frac{4\cdot 6^3}{K'}}\right]} = \frac{1}{[N_4]_{tot}}\cdot\Delta_0' \tag{B.40}$$

$$S = 8[N_4]_{tot}^3 K' \tag{B.41}$$

$$Z = \frac{1}{2}\sqrt{\frac{K}{3\cdot 4}\left(\frac{1}{[N_4]_{tot}}\cdot\Delta_0' - \frac{6}{[N_4]_{tot}K'\Delta_0'}\right)} = [N_4]_{tot}.\frac{1}{2}\sqrt{\frac{8K'}{3}\left(\Delta_0' - \frac{6}{K'\Delta_0'}\right)} = [N_4]_{tot}\cdot Z' \tag{B.42}$$

noting that the term p in Eq. (B.31) is null, and that Δ_0' and Z' symbols are included in Eq. (B.40) and Eq. (B.42), respectively, for simplification purposes.

By collecting all the terms obtained above, we can calculate the solution for Eq. (B.29) from Eq. (B.30)

$$[D] = x = -[N_4]_{tot}Z' + \frac{1}{2}\sqrt{-4([N_4]_{tot}Z')^2 + \frac{8[N_4]_{tot}^2 K'}{Z'}} = [N_4]_{tot}\cdot\left[-Z' + \sqrt{-(Z')^2 + \frac{2K'}{Z'}}\right] = [N_4]_{tot}\cdot D' \tag{B.43}$$

where D' indicates the contents enclosed by brackets.

Hence, by replacing K and $[D]$ according to Eqs. (B.37) and (B.43), respectively, the partition function Q in Eq. (B.28) becomes

$$Q = 1 + \frac{8K'}{(D')^3} \tag{B.44}$$

noting that the $[N_4]_{tot}$ terms are mutually deleted, whereas the population fractions f_{AM} and f_D are obtained as

$$f_{AM} = \frac{1}{Q} \text{ and } f_D = \frac{8K'}{(D')^3 Q} \tag{B.45}$$

and the temperature-dependent enthalpy variation involved in the process, expressed per mole of monomer, is obtained as

$$\Delta H(T) = f_D \cdot \Delta_{dd}H' \text{ with } \Delta_{dd}H' = \frac{\Delta H^{vH}}{4} \tag{B.46}$$

For this specific model, T_{diss} and ΔH^{vH} are the fitting parameters gathered under the D' term, and there is no dependence on protein concentration (please note that each grouping under symbols, namely K' and D', is free from the total protein concentration term).

Appendix C

Derivation of equations for the $N_n \leftrightarrow nM \leftrightarrow nD$ model

Analogously to the cases shown in Appendix B, we need to begin from arranging the partition function Q in terms of the lowest number possible of fitting parameters to obtain the $C_p(T)$ curve.

i) $N_2 \overset{K_{diss}}{\leftrightarrow} 2M \overset{K_d}{\leftrightarrow} 2D$

The partition function Q is given by Eq. (26) and becomes for $n = 2$

$$Q = 1 + \frac{K_{diss}}{2[M]} + \frac{K_{diss}K_d}{2[M]} \tag{C.1}$$

The $[M]$ term can be determined by merging the mass balance equation (Eq. (A.8)) and the corresponding relation for the equilibrium constant under the approximation of equality between the thermodynamic activities and the related molar concentration terms (Eq. (21))

$$\frac{n}{K_{diss}}[M]^n + (1 + K_d)[M] - n[N_n]_{tot} = 0 \tag{C.2}$$

that becomes for $n = 2$

$$\frac{2}{K_{diss}}[M]^2 + (1 + K_d)[M] - 2[N_2]_{tot} = 0 \tag{C.3}$$

with

$$[M] = \frac{-(1 + K_d) + \sqrt{(1 + K_d)^2 + 16\frac{[N_2]_{tot}}{K_{diss}}}}{4} \cdot K_{diss} \tag{C.4}$$

Both the equilibrium constants K_d and K_{diss} are dependent on temperature according to the van't Hoff equation:

$$K_d(T) = \exp\left[\frac{\Delta_d H'}{R}\left(\frac{1}{T_d} - \frac{1}{T}\right)\right] \tag{C.5}$$

being the value $K_d(T_d) = 1$ as a consequence of the definition of the denaturation temperature, and

$$K_{diss}(T) = K_{diss}(T_{diss}) \cdot \exp\left[\frac{\Delta H^{vH}}{R}\left(\frac{1}{T_{diss}} - \frac{1}{T}\right)\right] = K_{diss}(T_{diss}) \cdot K'_{diss} = 2[N_2]_{tot}\frac{1}{[1 + K_d(T_{diss})]^2} \cdot K'_{diss} = 2[N_2]_{tot} \cdot K''_{diss} \tag{C.6}$$

where $K_{diss}(T_{diss})$ is substituted according to Eq. (A.10) for $n = 2$, K'_{diss} is defined as the exponential term of Eq. (C.6), and $K''_{diss} = K'_{diss}/[1 + K_d(T_{diss})]^2$ term, gathered for the sake of simplicity.

By replacing K_{diss} in Eq. (C.4) with Eq. (C.6), we obtain

$$[M] = \frac{-(1 + K_d) + \sqrt{(1 + K_d)^2 + \frac{8}{K''_{diss}}}}{4} \cdot K_{diss} \tag{C.7}$$

and, by indicating the entire main fraction under the symbol M',

$$[M] = M' \cdot K_{diss} \tag{C.8}$$

Therefore, the partition function Q from Eq. C.1) becomes

$$Q = 1 + \frac{2[N_2]_{tot} \cdot K''_{diss}}{4M'[N_2]_{tot} \cdot K''_{diss}} + \frac{2[N_2]_{tot} \cdot K''_{diss}K_d}{4M'[N_2]_{tot} \cdot K''_{diss}} = 1 + \frac{1}{2M'} + \frac{K_d}{2M'} \tag{C.9}$$

noting that the $[N_2]_{tot}$ terms are mutually deleted, whereas the population fractions f_{AM}, f_M, and f_D are obtained as

$$f_{AM} = \frac{1}{Q};\ f_M = \frac{1}{2M'Q};\ f_D = \frac{K_d}{2M'Q} \tag{C.10}$$

and the temperature-dependent enthalpy variation involved in the process, expressed per mole of monomer, is obtained as

$$\Delta H(T) = f_M \cdot \Delta_{diss}H^\circ + f_D \cdot (\Delta_{diss}H^\circ + \Delta_d H^\circ) \text{ with } \Delta_{diss}H^\circ = \frac{\Delta H^{vH}}{2} \tag{C.11}$$

For this specific model, T_{diss}, ΔH^{vH}, T_d, and $\Delta_d H^\circ$ are the fitting parameters gathered under the M' term, and there is no dependence on protein concentration (please note that each grouping under symbols, namely K'_{diss}, K''_{diss}, and M', is free from the total protein concentration term).

ii) $N_3 \overset{K_{diss}}{\leftrightarrow} 3M \overset{K_d}{\leftrightarrow} 3D$

The partition function Q is given by Eq. (26) and becomes for $n = 3$

$$Q = 1 + \frac{K_{diss}}{3[M]^2} + \frac{K_{diss}K_d}{3[M]^2} \tag{C.12}$$

The $[M]$ term can be determined by merging the mass balance equation (Eqs. (A.8) and (C.2)) and the corresponding relation for the equilibrium constant under the approximation of equality between the thermodynamic activities and the related molar concentration terms (Eq. (21)). For $n = 3$, Eq. (C.2) becomes

$$\frac{3}{K_{diss}}[M]^3 + (1 + K_d)[M] - 3[N_3]_{tot} = 0 \tag{C.13}$$

Being Eq. (C.13) a third-order equation, we can consider that the analytical solution for the generic $ax^3 + bx^2 + cx + d = 0$ $(a \neq 0)$ is given by Eq. (B.14). Similarly to the case reported in Appendix B.*ii*, for Eq. (C.13), the p, q, and $\sqrt{\Delta}$ terms (the latter directly considered as square root for convenience) defined by Eqs. (B.15), (B.16), and (B.17), respectively, can be written as

$$p = \frac{(1 + K_d)K_{diss}}{3} \tag{C.14}$$

$$q = -[N_3]_{tot}K_{diss} \tag{C.15}$$

$$\sqrt{\Delta} = K_{diss}\sqrt{\frac{[N_3]_{tot}^2}{4} + \frac{(1 + K_d)^3 K_{diss}}{27^2}} \tag{C.16}$$

Considering that K_d depends on temperature according to Eq. (C.5), and that K_{diss} temperature-dependence is given by

$$K_{diss}(T) = K_{diss}(T_{diss}) \cdot \exp\left[\frac{\Delta H^{vH}}{R}\left(\frac{1}{T_{diss}} - \frac{1}{T}\right)\right] = K_{diss}(T_{diss}) \cdot K'_{diss} = \frac{27}{4}[N_3]_{tot}^2 \frac{1}{[1 + K_d(T_{diss})]^3} \cdot K'_{diss} = \frac{27}{4}[N_3]_{tot}^2 \cdot K''_{diss} \tag{C.17}$$

where $K_{diss}(T_{diss})$ is substituted according to Eq. (A.10) for $n = 3$, K'_{diss} is defined as the exponential term of Eq. (C.17), and $K''_{diss} = K'_{diss}/[1 + K_d(T_{diss})]^3$, gathered for the sake of simplicity, Eq. (C.16) can be further simplified by including Eq. (C.17):

$$\sqrt{\Delta} = K_{diss}\sqrt{\frac{[N_3]_{tot}^2}{4} + \frac{(1 + K_d)^3 \cdot [N_3]_{tot}^2 K''_{diss}}{27 \cdot 4}} = \frac{[N_3]_{tot}K_{diss}}{2}\sqrt{1 + \frac{(1 + K_d)^3 K''_{diss}}{27}} = \frac{[N_3]_{tot}K_{diss}}{2}\sqrt{\Delta'} \tag{C.18}$$

with Δ' indicating the radicand for simplicity.

Therefore, the analytical solution for Eq. (C.13) is

$$[M] = x = \sqrt[3]{\frac{[N_3]_{tot}K_{diss}}{2} + \frac{[N_3]_{tot}K_{diss}}{2}\sqrt{\Delta'}} + \sqrt[3]{\frac{[N_3]_{tot}K_{diss}}{2} - \frac{[N_3]_{tot}K_{diss}}{2}\sqrt{\Delta'}} = \sqrt[3]{\frac{[N_3]_{tot}K_{diss}}{2}(1 + \sqrt{\Delta'})} + \sqrt[3]{\frac{[N_3]_{tot}K_{diss}}{2}(1 - \sqrt{\Delta'})} \tag{C.19}$$

By including Eq. (C.17), we have

$$[M] = \sqrt[3]{\frac{3^3[N_3]_{tot}^3 K''_{diss}}{2^3}(1 + \sqrt{\Delta'})} + \sqrt[3]{\frac{3^3[N_3]_{tot}^3 K''_{diss}}{2^3}(1 - \sqrt{\Delta'})} = \frac{3[N_3]_{tot}}{2}\left[\sqrt[3]{K''_{diss}(1 + \sqrt{\Delta'})} + \sqrt[3]{K''_{diss}(1 - \sqrt{\Delta'})}\right] = \frac{3[N_3]_{tot}}{2} \cdot M' \tag{C.20}$$

where M' indicates the contents enclosed by brackets.

At last, by replacing K_{diss} and $[M]$ according to Eqs. (C.17) and (C.20), respectively, the partition function Q in Eq. (C.12) becomes

$$Q = 1 + \frac{K''_{diss}}{(M')^2} + \frac{K''_{diss}K_d}{(M')^2} \tag{C.21}$$

noting that the $[N_3]_{tot}$ terms are mutually deleted, whereas the population fractions f_{AM}, f_M, and f_D are obtained as

$$f_{AM} = \frac{1}{Q};\ f_M = \frac{K''_{diss}}{(M')^2 Q};\ f_D = \frac{K''_{diss}K_d}{(M')^2 Q} \tag{C.22}$$

and the temperature-dependent enthalpy variation involved in the process, expressed per mole of monomer, is obtained as

$$\Delta H(T) = f_M \cdot \Delta_{diss}H^{\circ} + f_D \cdot (\Delta_{diss}H^{\circ} + \Delta_d H^{\circ}) \text{ with } \Delta_{diss}H^{\circ} = \frac{\Delta H^{vH}}{3} \tag{C.23}$$

For this specific model, T_{diss}, ΔH^{vH}, T_d, and $\Delta_d H^{\circ}$ are the fitting parameters gathered under the M' term, and there is no dependence on protein concentration (please note that each grouping under symbols is free from the total protein concentration term).

iii) $N_4 \overset{K_{diss}}{\leftrightarrow} 4M \overset{K_d}{\leftrightarrow} 4D$

The partition function Q is given by Eq. (26) and becomes for $n = 4$

$$Q = 1 + \frac{K_{diss}}{4[M]^3} + \frac{K_{diss}K_d}{4[M]^3} \tag{C.24}$$

The $[M]$ term can be determined by merging the mass balance equation and the corresponding relation for the equilibrium constant under the approximation of equality between the thermodynamic activities and the related molar concentration terms, that finally provides Eq. (C.2). For $n = 4$, Eq. (C.2) becomes

$$\frac{4}{K_{diss}}[M]^4 + (1 + K_d)[M] - 4[N_4]_{tot} = 0 \tag{C.25}$$

Being Eq. (C.25) a fourth-order equation, we can consider that, among the four solutions available, the only valid analytical solution for the generic $ax^4 + bx^3 + cx^2 + dx + e = 0$ ($a \neq 0$) is given by Eq. (B.30).

Knowing that K_d depends on temperature according to Eq. (C.5), and that K_{diss} temperature-dependence is given by

$$K_{diss}(T) = K_{diss}(T_{diss}) \cdot \exp\left[\frac{\Delta H^{vH}}{R}\left(\frac{1}{T_{diss}} - \frac{1}{T}\right)\right] = K_{diss}(T_{diss}) \cdot K'_{diss} = 32[N_4]_{tot}^3 \frac{1}{[1 + K_d(T_{diss})]^4} \cdot K'_{diss} = 32[N_4]_{tot}^3 \cdot K''_{diss} \tag{C.26}$$

where $K_{diss}(T_{diss})$ is substituted according to Eq. (A.10) for $n = 4$, K'_{diss} is defined as the exponential term of Eq. (C.26), and $K''_{diss} = K'_{diss}/[1 + K_d(T_{diss})]^4$ term, gathered for the sake of simplicity, all the terms p, S, Z, Δ_0, q, and s for Eq.(C.25) (each defined by Eqs. (B.31) to (B.36), respectively) can be calculated:

$$s = \frac{27(1 + K_d)^2}{8[N_4]_{tot}^3 K''_{diss}} \tag{C.27}$$

$$q = -\frac{6}{[N_4]_{tot}^2 K''_{diss}} \tag{C.28}$$

$$\Delta_0 = \sqrt[3]{\frac{1}{2}\left\{\frac{27(1 + K_d)^2}{8[N_4]_{tot}^3 K''_{diss}} + \sqrt{\left[\frac{27(1 + K_d)^2}{8[N_4]_{tot}^3 K''_{diss}}\right]^2 + 4\left(\frac{6}{[N_4]_{tot}^2 K''_{diss}}\right)^3}\right\}} = \frac{1}{[N_4]_{tot}} \sqrt[3]{\frac{1}{2}\left\{\frac{27(1 + K_d)^2}{8K''_{diss}} + \frac{1}{K''_{diss}}\sqrt{\left[\frac{27(1 + K_d)^2}{8}\right]^2 + \frac{4 \cdot 6^3}{K''_{diss}}}\right\}} = \frac{1}{[N_4]_{tot}} \cdot \Delta'_0 \tag{C.29}$$

$$S = 8[N_4]_{tot}^3 K''_{diss}(1 + K_d) \tag{C.30}$$

$$Z = \frac{1}{2}\sqrt{\frac{K_{diss}}{3 \cdot 4}\left(\frac{1}{[N_4]_{tot}} \cdot \Delta'_0 - \frac{6}{[N_4]_{tot} K''_{diss} \Delta'_0}\right)} = [N_4]_{tot} \cdot \frac{1}{2}\sqrt{\frac{8K''_{diss}}{3}\left(\Delta'_0 - \frac{6}{K''_{diss}\Delta'_0}\right)} = [N_4]_{tot} \cdot Z' \tag{C.31}$$

noting that the term p in Eq. (B.31) is null, and that Δ'_0 and Z' symbols are included in Eq. (C.29) and Eq. (C.31), respectively, for simplification purposes.

By collecting all the terms obtained above, we can calculate the solution for Eq. (C.25) from Eq. (B.30)

$$[M] = x = -[N_4]_{tot} Z' + \frac{1}{2}\sqrt{-4([N_4]_{tot} Z')^2 + \frac{8[N_4]_{tot}^2 K''_{diss}(1 + K_d)}{Z'}} = [N_4]_{tot} \cdot \left[-Z' + \sqrt{-(Z')^2 + \frac{2K''_{diss}(1 + K_d)}{Z'}}\right] = [N_4]_{tot} \cdot M' \tag{C.32}$$

where M' indicates the contents enclosed by brackets.

Hence, by replacing K_{diss} and $[M]$ according to Eqs. (C.26) and (C.32), respectively, the partition function Q in Eq. (C.24) becomes

$$Q = 1 + \frac{8K''_{diss}}{(M')^3} + \frac{8K''_{diss}K_d}{(M')^3} \tag{C.33}$$

noting that the $[N_4]_{tot}$ terms are mutually deleted, whereas the population fractions f_{AM}, f_M, and f_D are obtained as

$$f_{AM} = \frac{1}{Q};\ f_M = \frac{8K''_{diss}}{(M')^3 Q};\ f_D = \frac{8K''_{diss}K_d}{(M')^3 Q} \tag{C.34}$$

and the temperature-dependent enthalpy variation involved in the process, expressed per mole of monomer, is obtained as

$$\Delta H(T) = f_M \cdot \Delta_{diss}H^{\circ} + f_D \cdot (\Delta_{diss}H^{\circ} + \Delta_d H^{\circ}) \text{ with } \Delta_{diss}H^{\circ} = \frac{\Delta H^{vH}}{4} \tag{C.35}$$

For this specific model, T_{diss}, ΔH^{vH}, T_d, and $\Delta_d H^{\circ}$ are the fitting parameters gathered under the M' term, and there is no dependence on protein concentration (please note that each grouping under symbols is free from the total protein concentration term).

Appendix D

Derivation of equations for the $N_n \leftrightarrow I_n \leftrightarrow nD$ model

Analogously to the cases shown in Appendices B and C, we need to begin from arranging the partition function Q in terms of the lowest number possible of fitting parameters to obtain the $C_p(T)$ curve.

i) $N_2 \overset{K_I}{\leftrightarrow} I_2 \overset{K}{\leftrightarrow} 2D$

The partition function Q is given by Eq. (41) and becomes for $n = 2$

$$Q = 1 + K_I + \frac{K_I K}{2[D]} \tag{D.1}$$

The $[D]$ term can be determined by merging the mass balance equation (Eq. (A.12)) and the corresponding relation for the equilibrium constant under the approximation of equality between the thermodynamic activities and the related molar concentration terms (Eq. (36))

$$n[N_n]_{tot} = \frac{n[D]^n}{K}\left(\frac{1}{K_I} + 1\right) + [D] \tag{D.2}$$

$$\frac{n(1+K_I)}{K_I K}[D]^n + [D] - n[N_n]_{tot} = 0 \tag{D.3}$$

that becomes for $n = 2$

$$\frac{2(1+K_I)}{K_I K}[D]^2 + [D] - 2[N_2]_{tot} = 0 \tag{D.4}$$

with

$$[D] = \frac{-1 + \sqrt{1 + 16[N_2]_{tot}\frac{1+K_I}{K_I K}}}{4(1+K_I)} \cdot K_I K \tag{D.5}$$

Considering that K_I depends on temperature analogously to Eq. (C.5), the temperature-dependence of K is given by

$$K(T) = K(T_{diss}) \cdot \exp\left[\frac{\Delta H^{vH}}{R}\left(\frac{1}{T_{diss}} - \frac{1}{T}\right)\right] = K(T_{diss}) \cdot K' = 2[N_2]_{tot}\frac{1 + K_I(T_{diss})}{K_I(T_{diss})} \cdot K' = 2[N_2]_{tot} \cdot K'' \tag{D.6}$$

where $K(T_{diss})$ is substituted according to Eq. (A.15) for $n = 2$, K' is defined as the exponential term of Eq. (D.6), and $K'' = K'[1 + K_I(T_{diss})] / K_I(T_{diss})$ term, gathered for the sake of simplicity.

By replacing K in Eq. (D.5) with Eq. (D.6), we obtain

$$[D] = \frac{-1 + \sqrt{1 + 8\frac{1+K_I}{K_I K''}}}{4(1+K_I)} \cdot K_I K \tag{D.7}$$

and, by gathering the entire fraction under the symbol D',

$$[D] = D' \cdot K_I K \tag{D.8}$$

Therefore, the partition function Q from Eq. (D.1) becomes

$$Q = 1 + K_I + \frac{2[N_2]_{tot} \cdot K_I K''}{4D'[N_2]_{tot} \cdot K_I K''} = 1 + K_I + \frac{1}{2D'} \tag{D.9}$$

noting that the $[N_2]_{tot}$ terms are mutually deleted, whereas the population fractions f_{NAM}, f_{IAM}, and f_D are obtained as

$$f_{NAM} = \frac{1}{Q};\ f_{IAM} = \frac{K_I}{Q};\ f_D = \frac{1}{2D'Q} \tag{D.10}$$

and the temperature-dependent enthalpy variation involved in the process, expressed per mole of monomer, is obtained as

$$\Delta H(T) = f_{IAM}\cdot\Delta_I H^\circ + f_D\cdot(\Delta_I H^\circ + \Delta_{dd}H^\circ) \text{ with } \Delta_{dd}H^\circ = \frac{\Delta H^{vH}}{2} \tag{D.11}$$

For this specific model, T_I (defined similarly to the denaturation temperature T_d for a simple $N \leftrightarrow D$ equilibrium), $\Delta_I H^\circ$, T_{diss}, and ΔH^{vH} are the fitting parameters gathered under the D' term, and there is no dependence on protein concentration (please note that each grouping under symbols, namely K', K'', and D', is free from the total protein concentration term).

ii) $N_3 \overset{K_I}{\leftrightarrow} I_3 \overset{K}{\leftrightarrow} 3D$

The partition function Q is given by Eq. (41) and becomes for $n = 3$

$$Q = 1 + K_I + \frac{K_I K}{3[D]^2} \tag{D.12}$$

The $[D]$ term can be determined by merging the mass balance equation (Eqs. (A.12) and (D.3)) and the corresponding relation for the equilibrium constant under the approximation of equality between the thermodynamic activities and the related molar concentration terms (Eq. (36)). For $n = 3$, Eq. (D.3) becomes

$$\frac{3(1+K_I)}{K_I K}[D]^3 + [D] - 3[N_3]_{tot} = 0 \tag{D.13}$$

Being Eq. (D.13) a third-order equation, we can consider that the analytical solution for the generic $ax^3 + bx^2 + cx + d = 0$ $(a \neq 0)$ is given by Eq. (B.14). Similarly to the case reported in Appendix B.*ii*, for Eq. (D.13), the p, q, and $\sqrt{\Delta}$ terms (the latter directly considered as square root for convenience) defined by Eqs. (B.15), (B.16), and (B.17), respectively, can be written as

$$p = 3\frac{1}{3}\cdot\frac{K_I K}{1+K_I} \tag{D.14}$$

$$q = -[N_3]_{tot}\frac{K_I K}{1+K_I} \tag{D.15}$$

$$\sqrt{\Delta} = \frac{K_I K}{1+K_I}\sqrt{\frac{[N_3]_{tot}^2}{4} + \frac{1}{27^2}\cdot\frac{K_I K}{1+K_I}} \tag{D.16}$$

Considering that K_I depends on temperature analogously to Eq. (C.5), and that K temperature-dependence is given by

$$K(T) = K(T_{diss})\cdot\exp\left[\frac{\Delta H^{vH}}{R}\left(\frac{1}{T_{diss}} - \frac{1}{T}\right)\right] = K(T_{diss})\cdot K' = \frac{27}{4}[N_3]_{tot}^2\frac{1+K_I(T_{diss})}{K_I(T_{diss})}\cdot K' = \frac{27}{4}[N_3]_{tot}^2\cdot K'' \tag{D.17}$$

where $K(T_{diss})$ is substituted according to Eq. (A.15) for $n = 3$, K' is defined as the exponential term of Eq. (D.17), and $K'' = K'[1+K_I(T_{diss})]\,/K_I(T_{diss})$ term, gathered for the sake of simplicity, Eq. (D.16) can be further simplified by including Eq. (D.17):

$$\sqrt{\Delta} = \frac{K_I K}{1+K_I}\sqrt{\frac{[N_3]_{tot}^2}{4} + \frac{[N_3]_{tot}^2 K''}{27\cdot 4}\left(\frac{K_I}{1+K_I}\right)} = \frac{[N_3]_{tot}}{2}\left(\frac{K_I K}{1+K_I}\right)\sqrt{1 + \frac{K''}{27}\left(\frac{K_I}{1+K_I}\right)} = \frac{[N_3]_{tot}}{2}\left(\frac{K_I K}{1+K_I}\right)\sqrt{\Delta'} \tag{D.18}$$

with Δ' indicating the radicand for simplicity.

Therefore, the analytical solution for Eq. (D.13) is

$$\begin{aligned}[D] = x &= \sqrt[3]{\frac{[N_3]_{tot}}{2}\left(\frac{K_I K}{1+K_I}\right) + \frac{[N_3]_{tot}}{2}\left(\frac{K_I K}{1+K_I}\right)\sqrt{\Delta'}} + \sqrt[3]{\frac{[N_3]_{tot}}{2}\left(\frac{K_I K}{1+K_I}\right) - \frac{[N_3]_{tot}}{2}\left(\frac{K_I K}{1+K_I}\right)\sqrt{\Delta'}} \\ &= \sqrt[3]{\frac{[N_3]_{tot}}{2}\left(\frac{K_I K}{1+K_I}\right)(1+\sqrt{\Delta'})} + \sqrt[3]{\frac{[N_3]_{tot}}{2}\left(\frac{K_I K}{1+K_I}\right)(1-\sqrt{\Delta'})}\end{aligned} \tag{D.19}$$

By including Eq. (D.17), we have

$$[D] = \sqrt[3]{\frac{3^3[N_3]_{tot}^3 K''}{2^3}\left(\frac{K_I}{1+K_I}\right)(1+\sqrt{\Delta'})} + \sqrt[3]{\frac{3^3[N_3]_{tot}^3 K''}{2^3}\left(\frac{K_I}{1+K_I}\right)(1-\sqrt{\Delta'})} = \frac{3[N_3]_{tot}}{2}\left[\sqrt[3]{\frac{K_I K''}{1+K_I}(1+\sqrt{\Delta'})} + \sqrt[3]{\frac{K_I K''}{1+K_I}(1-\sqrt{\Delta'})}\right] = \frac{3[N_3]_{tot}}{2}\cdot D' \tag{D.20}$$

where D' indicates the contents enclosed by brackets.

At last, by replacing K and $[D]$ according to Eqs. (D.17) and (D.20), respectively, the partition function Q in Eq. (D.12) becomes

$$Q = 1 + K_I + \frac{K_I K''}{(D')^2} \tag{D.21}$$

noting that the $[N_3]_{tot}$ terms are mutually deleted, whereas the population fractions f_{NAM}, f_{IAM}, and f_D are obtained as

$$f_{NAM} = \frac{1}{Q};\ f_{IAM} = \frac{K_I}{Q};\ f_D = \frac{K_I K''}{(D')^2 Q} \tag{D.22}$$

and the temperature-dependent enthalpy variation involved in the process, expressed per mole of monomer, is obtained as

$$\Delta H(T) = f_{IAM}\cdot\Delta_I H^\circ + f_D\cdot(\Delta_I H^\circ + \Delta_{dd} H^\circ) \text{ with } \Delta_{dd} H^\circ = \frac{\Delta H^{vH}}{3} \tag{D.23}$$

For this specific model, T_I (defined similarly to the denaturation temperature T_d for a simple $N \leftrightarrow D$ equilibrium), $\Delta_I H^\circ$, T_{diss}, and ΔH^{vH} are the fitting parameters gathered under the D' term, and there is no dependence on protein concentration (please note that each grouping under symbols, namely K', K'', and D', is free from the total protein concentration term).

iii) $N_4 \overset{K_I}{\leftrightarrow} I_4 \overset{K}{\leftrightarrow} 4D$

The partition function Q is given by Eq. (41) and becomes for $n = 4$

$$Q = 1 + K_I + \frac{K_I K}{4[D]^3} \tag{D.24}$$

The $[D]$ term can be determined by merging the mass balance equation and the corresponding relation for the equilibrium constant under the approximation of equality between the thermodynamic activities and the related molar concentration terms, that finally provides Eq. (D.3). For $n = 4$, Eq. (D.3) becomes

$$\frac{4(1+K_I)}{K_I K}[D]^4 + [D] - 4[N_4]_{tot} = 0 \tag{D.25}$$

Being Eq. (D.25) a fourth-order equation, we can consider that, among the four solutions available, the only valid analytical solution for the generic $ax^4 + bx^3 + cx^2 + dx + e = 0$ ($a \neq 0$) is given by Eq. (B.30).

Knowing that K_I depends on temperature analogously to Eq. (C.5), and that K temperature-dependence is given by

$$K(T) = K(T_{diss})\cdot\exp\left[\frac{\Delta H^{vH}}{R}\left(\frac{1}{T_{diss}} - \frac{1}{T}\right)\right] = K(T_{diss})\cdot K' = 32[N_4]^3_{tot}\frac{1+K_I(T_{diss})}{K_I(T_{diss})}\cdot K' = 32[N_4]^3_{tot}\cdot K'' \tag{D.26}$$

where $K(T_{diss})$ is substituted according to Eq. (A.15) for $n = 4$, K' is defined as the exponential term of Eq. (D.26), and $K''_{diss} = K'[1+K_I(T_{diss})]\,/K_I(T_{diss})$ term, gathered for the sake of simplicity, all the terms p, S, Z, Δ_0, q, and s for Eq. (D.25) (each defined by Eqs. (B.31) to (B.36), respectively) can be calculated:

$$s = \frac{27}{8[N_4]^3_{tot}}\left(\frac{1+K_I}{K_I K''}\right) \tag{D.27}$$

$$q = -\frac{6}{[N_4]^2_{tot}}\left(\frac{1+K_I}{K_I K''}\right) \tag{D.28}$$

$$\Delta_0 = \sqrt[3]{\frac{1}{2}\left\{\frac{27}{8[N_4]^3_{tot}}\left(\frac{1+K_I}{K_I K''}\right) + \sqrt{\left[\frac{27}{8[N_4]^3_{tot}}\left(\frac{1+K_I}{K_I K''}\right)\right]^2 + 4\left[\frac{6}{[N_4]^2_{tot}}\left(\frac{1+K_I}{K_I K''}\right)\right]^3}\right\}} = \frac{1}{[N_4]_{tot}}\sqrt[3]{\frac{1}{2}\left(\frac{1+K_I}{K_I K''}\right)\left[\frac{27}{8} + \sqrt{\left(\frac{27}{8}\right)^2 + 4\cdot 6^3\left(\frac{1+K_I}{K_I K''}\right)}\right]} = \frac{1}{[N_4]_{tot}}\cdot\Delta_0' \tag{D.29}$$

$$S = 8[N_4]^3_{tot}\left(\frac{K_I K''}{1+K_I}\right) \tag{D.30}$$

$$Z = \frac{1}{2}\sqrt{\frac{1}{3\cdot 4}\left(\frac{K_I K}{1+K_I}\right)\left[\frac{\Delta_0'}{[N_4]_{tot}} - \frac{6}{[N_4]_{tot}\Delta_0'}\left(\frac{1+K_I}{K_I K''}\right)\right]} = [N_4]_{tot}\cdot\frac{1}{2}\sqrt{\frac{8}{3}\left(\frac{K_I K''}{1+K_I}\right)\left[\Delta_0' - \frac{6}{\Delta_0'}\left(\frac{1+K_I}{K_I K''}\right)\right]} = [N_4]_{tot}\cdot Z' \tag{D.31}$$

noting that the term p in Eq. (B.31) is null, and that Δ_0' and Z' symbols are included in Eq. (D.29) and Eq. (D.31), respectively, for simplification purposes.

By collecting all the terms obtained above, we can calculate the solution for Eq. (D.25) from Eq. (B.30)

$$[D] = x = -[N_4]_{tot}Z' + \frac{1}{2}\sqrt{-4([N_4]_{tot}Z')^2 + \frac{8[N_4]^2_{tot}}{Z'}\left(\frac{K_I K''}{1+K_I}\right)} = [N_4]_{tot}\cdot\left[-Z' + \sqrt{-(Z')^2 + \frac{2}{Z'}\left(\frac{K_I K''}{1+K_I}\right)}\right] = [N_4]_{tot}\cdot D' \tag{D.32}$$

where D' indicates the contents enclosed by brackets.

Hence, by replacing K and $[D]$ according to Eqs. (D.26) and (D.32), respectively, the partition function Q in Eq. (D.24) becomes

$$Q = 1 + K_I + \frac{8K_I K''}{(D')^3} \tag{D.33}$$

noting that the $[N_4]_{tot}$ terms are mutually deleted, whereas the population fractions f_{NAM}, f_{IAM}, and f_D are obtained as

$$f_{NAM} = \frac{1}{Q};\ f_{IAM} = \frac{K_I}{Q};\ f_D = \frac{8K_IK''}{(D')^3Q} \tag{D.34}$$

and the temperature-dependent enthalpy variation involved in the process, expressed per mole of monomer, is obtained as

$$\Delta H(T) = f_{IAM}\cdot\Delta_I H^\circ + f_D\cdot(\Delta_I H^\circ + \Delta_{dd}H^\circ) \text{ with } \Delta_{dd}H^\circ = \frac{\Delta H^{vH}}{4} \tag{D.35}$$

For this specific model, T_I (defined similarly to the denaturation temperature T_d for a simple $N \leftrightarrow D$ equilibrium), $\Delta_I H^\circ$, T_{diss}, and ΔH^{vH} are the fitting parameters gathered under the D' term, and there is no dependence on protein concentration (please note that each grouping under symbols, namely K', K'', and D', is free from the total protein concentration term).

Appendix E

Obtaining the theoretical $C_p(T)$ from the models' solutions on a spreadsheet

As emerges from Appendices B, C, and D, the development of the models always allows to achieve very specific expressions for the $\Delta H(T)$ function that finally include all the fitting parameters needed. Hence, the temperature-derivative of $\Delta H(T)$ function

$$C_p(T) = \frac{d\Delta H(T)}{dT} \tag{E.1}$$

provides the theoretical $C_p(T)$ curve for the fitting of the experimental DSC thermograms.

If for the simplest case of a monomeric protein denaturation equilibrium the development of the derivative in Eq. (E.1) can produce the explicit $C_p(T)$ function straightforwardly [30,31], the same procedure applied to the equations determined above might be unnecessarily troublesome. Consequently, it is more practical to obtain the $C_p(T)$ function by numerical derivation of the $\Delta H(T)$ function either by means of a suitable software or alternatively through the simple general equation for x_i, y_i columns on a spreadsheet

$$\frac{dy(x)}{dx} = \frac{y_{i+1} - y_i}{x_{i+1} - x_i} \tag{E.2}$$

In other words, the graphical representation of the theoretical $C_p(T)$ profile can be obtained through

$$C_p(T) = \frac{d\Delta H(T)}{dT} = \frac{\Delta H(T)_{i+1} - \Delta H(T)_i}{T_{i+1} - T_i} \tag{E.3}$$

being careful to set the T column with small temperature steps (for instance, with ΔT steps no wider than 0.1 K).

Such a theoretical representation can thus be compared to the experimental data, that need to be represented in terms of $C_p^{exc}(T)$ (normalized per mole of protein monomer and in excess with respect to the native state), a physical quantity that is the result of raw data treatments. In this context, it is worth recalling that a raw calorimetric signal may be shown as Heat Flow (HF) or Power (P) depending on the calorimeter type used (but always reporting the difference of the heat flow between the sample and the reference cells). In any case, the calorimetric signal is just

$$\text{signal} = HF \text{ (or } P) = \frac{\mathrm{d}Q}{\mathrm{d}t} \tag{E.4}$$

with Q as heat and t as time, whose unit is a multiple or submultiple of Watt if Q is expressed in Joules and t is expressed in seconds.

Considering that Q corresponds to the thermodynamic state function enthalpy H when at constant pressure ($\mathrm{d}Q = \mathrm{d}H$), by multiplying the signal by the conversion factor $f = 1/(\beta\cdot n)$, where $\beta = \mathrm{d}T/\mathrm{d}t$ is the scanning rate of the DSC measurement considered and n is the number of monomer moles, HF can be easily converted into an apparent specific heat capacity at constant pressure, C_p^{app}

$$HF\cdot\frac{1}{\beta}\frac{1}{n} = \frac{\mathrm{d}H}{\mathrm{d}t}\cdot\frac{\mathrm{d}t}{\mathrm{d}T}\cdot\frac{1}{n} = C_p^{app} \tag{E.5}$$

In turn, C_p^{exc} can be obtained from C_p^{app} by coherent baseline subtraction. This procedure is crucial for any globular protein (both monomeric and multimeric) thermal denaturation experiment, and literature reports many works related, including ours devoted to this issue. In particular, for the experiments shown in this work, we followed the procedure proposed and described in details in our previous works [30,36]. Briefly, the subtraction of a first baseline obtained from buffer-buffer experiment is recommended. Concerning the treatment of pre-/post-denaturation region, criteria for a proper baseline choice are discussed to detect the onset/offset temperatures of the thermal transition as well as to obtain the overall intrinsic heat capacity drop $\Delta_d C_p$ between the native and final denatured state.

As a matter of fact, the $\Delta_d C_p$ is often too small compared to the calorimetric denaturation peak. Hence, in spite of precautions, it may be affected by rather large errors during baseline treatment that might compromise the theoretical modelling even further. For this reason, a third sigmoidal baseline is used, throughout the peak temperature range, that distributes the $C_p(T_f) - C_p(T_i)$ difference according to the evolution (degree of advancement) of the calorimetric peak. We observed that this procedure reduces the potential error of the $\Delta_d C_p$ value and produces only almost negligible effects on the profile of the final experimental the $C_p^{exc}(T)$ curve to be used for the fitting procedure of the theoretical models.

We may say that when dealing with multiple protein thermal events, such as protein dissociation and denaturation, recovering information on the $\Delta_d C_p$ drop distribution for each event is possible for each model only after obtaining the species fractions if simple additivity can be assumed to obtain the overall $\Delta_d C_p$ drop. However, the $\Delta_d C_p$ depends on entropic factors as well as on the accessible surface area to the solvent, and additivity is not guaranteed. These details depend on the peculiar system and cannot be generalized. This is the second reason (to be added to the experimental uncertainty) that the $\Delta_d C_p$ is not further exploited in this work (this is almost the case also for many theoretical models for monomers).

Data availability

Data will be made available on request.

References

[1] D. Whitford, Proteins: Structure and Function, John Wiley & Sons, 2013.
[2] N.E. Hynes, H.A. Lane, ERBB receptors and cancer: the complexity of targeted inhibitors, Nat. Rev. Cancer 5 (2005) 341–354, https://doi.org/10.1038/nrc1609.
[3] T.L. Spires-Jones, J. Attems, D.R. Thal, Interactions of pathological proteins in neurodegenerative diseases, Acta Neuropathol. 134 (2017) 187–205, https://doi.org/10.1007/s00401-017-1709-7.
[4] N.G. Herrera, N.C. Morano, A. Celikgil, G.I. Georgiev, R.J. Malonis, J.H. Lee, K. Tong, O. Vergnolle, A.B. Massimi, L.Y. Yen, A.J. Noble, M. Kopylov, J. B. Bonanno, S.C. Garrett-Thomson, D.B. Hayes, R.H. Bortz, A.S. Wirchnianski, C. Florez, E. Laudermilch, D. Haslwanter, J.M. Fels, M.E. Dieterle, R.K. Jangra, J. Barnhill, A. Mengotto, D. Kimmel, J.P. Daily, L. Pirofski, K. Chandran, M. Brenowitz, S.J. Garforth, E.T. Eng, J.R. Lai, S.C. Almo, Characterization of the SARS-CoV-2 S protein: biophysical, biochemical, structural, and antigenic analysis, ACS. Omega 6 (2021) 85–102, https://doi.org/10.1021/acsomega.0c03512.
[5] S.M. Iyengar, K.K. Barnsley, H.Y. Vu, I.J.A. Bongalonta, A.S. Herrod, J.A. Scott, M. J. Ondrechen, Identification and characterization of alternative sites and molecular probes for SARS-CoV-2 target proteins, Front. Chem. 10 (2022) 1017394, https://doi.org/10.3389/fchem.2022.1017394.
[6] A. Gaber, M. Pavšič, Modeling and structure determination of homo-oligomeric proteins: an overview of challenges and current approaches, Int. J. Mol. Sci. 22 (2021) 9081, https://doi.org/10.3390/ijms22169081.
[7] A. Venturelli, G. Guaitoli, D. Vanossi, F. Saitta, D. Fessas, S. Vitiello, G. Malpezzi, D. Aiello, S. Ferrari, D. Tondi, G. Ponterini, M.Paola Costi, Intersite communication in dimeric enzymes highlighted by structural and thermodynamic analysis of didansyltyrosine binding to thymidylate synthases, Bioorg. Chem. 151 (2024) 107663, https://doi.org/10.1016/j.bioorg.2024.107663.
[8] P.G.V. Liggri, K.E. Tsitsanou, E.C.V. Stamati, F. Saitta, C.E. Drakou, D.D. Leonidas, D. Fessas, S.E. Zographos, The structure of AgamOBP5 in complex with the natural insect repellents Carvacrol and Thymol: crystallographic, fluorescence and thermodynamic binding studies, Int. J. Biol. Macromol. 237 (2023) 124009, https://doi.org/10.1016/j.ijbiomac.2023.124009.
[9] P.M. Wiggins, Hydrophobic hydration, hydrophobic forces and protein folding, Phys. A Stat. Mech. Its Appl. 238 (1997) 113–128, https://doi.org/10.1016/S0378-4371(96)00431-1.
[10] N. Perunov, J.L. England, Quantitative theory of hydrophobic effect as a driving force of protein structure, Protein Sci. 23 (2014) 387–399, https://doi.org/10.1002/pro.2420.
[11] S.J. Hubbard, K.-H. Gross, P. Argos, Intramolecular cavities in globular proteins, Protein Eng. Des. Sel. 7 (1994) 613–626, https://doi.org/10.1093/protein/7.5.613.
[12] M.A. Williams, J.M. Goodfellow, J.M. Thornton, Buried waters and internal cavities in monomeric proteins, Protein Sci. 3 (1994) 1224–1235, https://doi.org/10.1002/pro.5560030808.
[13] G. Guaitoli, X. Zhang, F. Saitta, P. Miglionico, L.M. Silbermann, F.Y. Ho, F. von Zweydorf, M. Signorelli, K. Tych, D. Fessas, F. Raimondi, A. Kortholt, C. J. Gloeckner, Biophysical analysis reveals autophosphorylation as an important negative regulator of LRRK2 dimerization, bioRxiv. 2023 (2023), https://doi.org/10.1101/2023.08.11.549911, 08.11.549911.
[14] F. Saitta, J. Masuri, M. Signorelli, S. Bertini, A. Bisio, D. Fessas, Thermodynamic insights on the effects of low-molecular-weight heparins on antithrombin III, Thermochim. Acta 713 (2022) 179248, https://doi.org/10.1016/j.tca.2022.179248.
[15] D. Fessas, S. Iametti, A. Schiraldi, F. Bonomi, Thermal unfolding of monomeric and dimeric β-lactoglobulins, Eur. J. Biochem. 268 (2001) 5439–5448, https://doi.org/10.1046/j.0014-2956.2001.02484.x.
[16] G. Mei, A. Di Venere, N. Rosato, A. Finazzi-Agrò, The importance of being dimeric, FEBS. J. 272 (2005) 16–27, https://doi.org/10.1111/j.1432-1033.2004.04407.x.
[17] E.D. Levy, S.A. Teichmann, Structural, evolutionary, and Assembly Principles of protein oligomerization, in: Prog. Mol. Biol. Transl. Sci., Academic Press, 2013, pp. 25–51, https://doi.org/10.1016/B978-0-12-386931-9.00002-7.
[18] J.A. Marsh, H.A. Rees, S.E. Ahnert, S.A. Teichmann, Structural and evolutionary versatility in protein complexes with uneven stoichiometry, Nat. Commun. 6 (2015) 6394, https://doi.org/10.1038/ncomms7394.
[19] J. Monod, J. Wyman, J.-P. Changeux, On the nature of allosteric transitions: a plausible model, J. Mol. Biol. 12 (1965) 88–118, https://doi.org/10.1016/S0022-2836(65)80285-6.
[20] R.A. Cook, D.E. Koshland, Specificity in the assembly of multisubunit proteins, Proc. Natl. Acad. Sci. 64 (1969) 247–254, https://doi.org/10.1073/pnas.64.1.247.
[21] M.H. Ali, B. Imperiali, Protein oligomerization: how and why, Bioorg. Med. Chem. 13 (2005) 5013–5020, https://doi.org/10.1016/j.bmc.2005.05.037.
[22] P.L. Privalov, N.N. Khechinashvili, A thermodynamic approach to the problem of stabilization of globular protein structure: a calorimetric study, J. Mol. Biol. 86 (1974) 665–684, https://doi.org/10.1016/0022-2836(74)90188-0.
[23] E. Freire, R.L. Biltonen, Statistical mechanical deconvolution of thermal transitions in macromolecules. II. General treatment of cooperative phenomena, Biopolymers 17 (1978) 481–496, https://doi.org/10.1002/bip.1978.360170213.
[24] R.L. Biltonen, E. Freire, J.F. Brandts, Thermodynamic characterization of conformational states of biological macromolecules using differential scanning calorimetry, CRC Crit. Rev. Biochem. 5 (1978) 85–124, https://doi.org/10.3109/10409237809177141.
[25] P.L. Privalov, S.A. Potekhin, [2]Scanning microcalorimetry in studying temperature-induced changes in proteins, Methods Enzymol. (1986) 4–51, https://doi.org/10.1016/0076-6879(86)31033-4.
[26] F. Saitta, P. Cannazza, S. Donzella, V. De Vitis, M. Signorelli, D. Romano, F. Molinari, D. Fessas, Calorimetric and thermodynamic analysis of an enantioselective carboxylesterase from Bacillus coagulans: insights for an industrial scale-up, Thermochim. Acta 713 (2022) 179247, https://doi.org/10.1016/j.tca.2022.179247.
[27] C. Pelosi, F. Saitta, F.R. Wurm, D. Fessas, M.R. Tinè, C. Duce, Thermodynamic stability of myoglobin-poly(ethylene glycol) bioconjugates: a calorimetric study, Thermochim. Acta 671 (2019) 26–31, https://doi.org/10.1016/j.tca.2018.11.001.
[28] S. Marciano, D. Dey, D. Listov, S.J. Fleishman, A. Sonn-Segev, H. Mertens, F. Busch, Y. Kim, S.R. Harvey, V.H. Wysocki, G. Schreiber, Protein quaternary structures in solution are a mixture of multiple forms, Chem. Sci. 13 (2022) 11680–11695, https://doi.org/10.1039/D2SC02794A.
[29] J.A.O. Rumfeldt, C. Galvagnion, K.A. Vassall, E.M. Meiering, Conformational stability and folding mechanisms of dimeric proteins, Prog. Biophys. Mol. Biol. 98 (2008) 61–84, https://doi.org/10.1016/j.pbiomolbio.2008.05.004.
[30] G. Barone, P. Del Vecchio, D. Fessas, C. Giancola, G. Graziano, Denaturation of biological macromolecules: new programs for the deconvolution of DSC measurements, (1994) 67–78. doi:10.1007/978-94-011-0822-5_7.
[31] G. Barone, F. Catanzano, P. Del Vecchio, D. Fessas, C. Giancola, G. Graziano, The effect of pH on thermal stability of globular proteins, J. Therm. Anal. 42 (1994) 383–395, https://doi.org/10.1007/BF02548523.
[32] A. Ausili, A. Pennacchio, M. Staiano, J.D. Dattelbaum, D. Fessas, A. Schiraldi, S. D'Auria, Amino acid transport in thermophiles: characterization of an arginine-binding protein from Thermotoga maritima. 3. Conformational dynamics and stability, J. Photochem. Photobiol. B Biol. 118 (2013) 66–73, https://doi.org/10.1016/j.jphotobiol.2012.11.004.
[33] J.R. Lepock, K.P. Ritchie, M.C. Kolios, A.M. Rodahl, K.A. Heinz, J. Kruuv, Influence of transition rates and scan rate on kinetic simulations of differential scanning calorimetry profiles of reversible and irreversible protein denaturation, Biochemistry 31 (1992) 12706–12712, https://doi.org/10.1021/bi00165a023.
[34] M.H. Sleiman, R. Csonka, C. Arbez-Gindre, G.A. Heropoulos, T. Calogeropoulou, M. Signorelli, A. Schiraldi, B.R. Steele, D. Fessas, M. Micha-Screttas, Binding and stabilisation effects of glycodendritic compounds with peanut agglutinin, Int. J. Biol. Macromol. 80 (2015) 692–701, https://doi.org/10.1016/j.ijbiomac.2015.07.036.
[35] S.K. Natchiar, K. Suguna, A. Surolia, M. Vijayan, Peanut agglutinin, a lectin with an unusual quaternary structure and interesting ligand binding properties, Crystallogr. Rev. 13 (2007) 3–28, https://doi.org/10.1080/08893110701382087.
[36] G. Barone, P. Del Vecchio, D. Fessas, C. Giancola, G. Graziano, Theseus: a new software package for the handling and analysis of thermal denaturation data of biological macromolecules, J. Therm. Anal. 38 (1992) 2779–2790, https://doi.org/10.1007/BF01979752.